10-18-2019

Dinaciclib Inhibits Glioblastoma Multiforme Cell Growth and Selects for a Brain Tumour Initiating Cell Population

Mathew Stover
University of Windsor

Dinaciclib Inhibits Glioblastoma Multiforme Cell Growth and Selects for a Brain Tumour Initiating Cell Population

By

Mathew Stover

A Thesis
Submitted to the Faculty of Graduate Studies
through the Department of Biomedical Sciences
in Partial Fulfillment of the Requirements for
the Degree of Master of Science
at the University of Windsor

Windsor, Ontario, Canada

2019

Dinaciclib Inhibits Glioblastoma Multiforme Cell Growth and Selects for a Brain Tumour Initiating Cell Population

by

Mathew Stover

APPROVED BY:

_____

J. Trant
Department of Chemistry and Biochemistry

_____

H. Zhang
Department of Biomedical Sciences

_____

L. Porter, Advisor
Department of Biomedical Sciences

October 16, 2019

DECLARATION OF CO-AUTHORSHIP

I hereby declare that this thesis incorporates material that is result of joint research, as follows:

This thesis incorporates the outcome of joint research undertaken in collaboration with Janice Tubman under the supervision of Dr. Lisa Porter. This collaboration is covered in Figures 1 and 8 of this thesis. The images, data analysis, statistical analysis, graphing results, interpretation, and writing were performed by the author, and the contribution of Janice Tubman was by providing images for analysis in Figure 8C. Janice Tubman also provided the image for Figure 1A.

I am aware of the University of Windsor Senate Policy on Authorship and I certify that I have properly acknowledged the contribution of other researchers to my thesis and have obtained written permission from each of the co-author(s) to include the above material(s) in my thesis.

I certify that, with the above qualification, this thesis, and the research to which it refers, is the product of my own work.

I certify that, to the best of my knowledge, my thesis does not infringe upon anyone's copyright nor violate any proprietary rights and that any ideas, techniques, quotations, or any other material from the work of other people included in my thesis, published or otherwise, are fully acknowledged in accordance with the standard referencing practices. Furthermore, to the extent that I have included copyrighted material that surpasses the bounds of fair dealing within the meaning of the Canada Copyright Act, I certify that I have obtained a written permission from the copyright owner(s) to include such material(s) in my thesis and have included copies of such copyright clearances to my appendix.

I declare that this is a true copy of my thesis, including any final revisions, as approved by my thesis committee and the Graduate Studies office, and that this thesis has not been submitted for a higher degree to any other University or Institution.

ABSTRACT

Glioblastoma Multiforme (GBM) is a highly aggressive and devastating primary brain tumour with a prognosis of 12-15 months with standard of care treatments, which includes combinations of surgery, radiotherapy and chemotherapy. Aggressiveness, among other factors, is driven by the populations of brain tumour initiating cells, capable of self renewal, tumour recapitulation and high therapy resistance. Dinaciclib is a potent cyclin-dependent kinase (CDK) inhibitor (CKI) which inhibits GBM cell growth *in vitro*. This study confirmed the growth inhibition of GBM cells but also demonstrated enrichment for specific brain tumour initiating cell populations upon dinaciclib treatment. In the zebrafish (*Danio rerio*) model, dinaciclib showed less toxicity to the developing embryos than NU2058, another CKI with similar CDK targets. Embryos injected with U87 cells, a GBM cell line, were treated with dinaciclib and we demonstrated that there was a decrease in cell foci area after treatment with dinaciclib compared to the vehicle control. The breast cancer cells, MDA-MB-231, were also injected into zebrafish embryos to perform a comparative analysis of spatial trends in cell metastasis. Interestingly, there appears to be a preferential migration of injected cancer cells to the organ of cancer origin, with GBM cells migrating towards the brain and head and breast cancer cells migrating down the tail. In summary, we demonstrated that using a CKI simultaneously with a chemotherapy induces antagonistic effects in GBM cells, which demonstrates the importance of timing of drug administration in the clinic.

ACKNOWLEDGEMENTS

I would like to start my acknowledgements with Dr. Lisa Porter, who has been extremely patient and kind, and was willing to give me the opportunity to obtain this Master's degree, thank you.

I would like to thank my committee members, Dr. Huiming Zhang and Dr. John Trant, for their time, advice, and review of this work.

A critical acknowledgement goes out to Dr. Dorota Lubanska, for her guidance and support. You are incredibly kind and generous, and this degree would not be possible without you, thank you.

I would like to acknowledge Janice Tubman and Martin Bakht. Janice for her help all things zebrafish, injections and image analysis included. Martin for his general guidance and advice throughout this degree. I would not have accomplished this feat without the two of you, thank you.

I would like to thank Dr. Bre-Anne Fifield and Dr. Elizabeth Fidalgo da Silva for their direct help with me at times and for the everyday work they do to maintain the lab.

I would like to acknowledge Dr. Keith Frank Stringer, to which I have been a bad "wing-man" and I would like to officially apologize for that. Frank is a hard worker, punctual, and puts in more hours in the lab than anyone else I know (aside from maybe Martin). Buy Bitcoin.

Thank you to the rest of the Porter Lab group, everyone has tolerated my shenanigans beyond my own expectations, cheers.

TABLE OF CONTENTS

LIST OF TABLES

LIST OF FIGURES

LIST OF ABBREVIATIONS/SYMBOLS

ABC……..……..……ATP-binding cassette

AML……...… acute myeloid leukemia

ATM……..…….ataxia-telangiectasia-mutated

BBB……..……...blood-brain barrier

BCNU……..…bis-chloroethylnitrosourea

BTIC……..…….brain tumour initiating cell

CC-3……..……...…….cleaved caspase-3

CD……...……...cluster of differentiation

CDK...…….……..……..cyclin-dependent kinase

CEC……...……cerebrovascular endothelial cells

Chk1……..……...……..checkpoint kinase 1

Chk2……..…….……checkpoint kinase 2

CKI……..……...……..cyclin-dependent kinase inhibitor

CNS.……..……central nervous system

CSC……..cancer stem cell

CSF……..……..……..cerebrospinal fluid

dpf…….……..……..……..days post-fertilization

DMEM……...……..……..Dulbecco’s modified Eagle’s medium

DMSO……..……..……..dimethyl sulfoxide

EC_{50}……..…….……..half maximal effective concentration

EMEM…….…….……Eagle's minimum essential medium

ESA……..……..……...epithelial specific antigen

FBS……..……..…fetal bovine serum

FDA……..……...The US Food and Drug Administration

FOV……..…….field of view

HBSS……..……Hanks Balanced Salt Solution

hpf……..……..……..hours post fertilization

G_0……...……non-growth phase

G_1……...……..……..……gap 1

G_2……...……..…..gap 2

GBM……...……...….…glioblastoma multiforme

GSC……..……...……glioma stem-cell

IC_{50} ……...……..……...…….inhibitory concentration of 50%

K_i……..……..…the inhibitory constant

M……..…….….mitosis

MAP2……...…..microtubule associated protein 2

MTIC……...……...3-methyl-(triazen-1-yl) imidazole-4-carboxamide

MTT…….……...Thiazolyl Blue Tetrazolium Bromide

PBS….……..…..……...phosphate buffered solution

PCR…….……..…...polymerase chain reaction

PFA……..…….…….……paraformaldehyde

qRT-PCR……..……...…….Quantitative Real-Time polymerase chain reaction

RINGO……...… Rapid Inducer of G_2/M Progression in Oocytes

RQ……..…….……...……..relative quantification

S……...……..…..synthesis

Spy1…….……...……Spy1A

TMZ……..……..temozolomide

WHO……...…….……..World Health Organization

WT..……wild-type

INTRODUCTION

1. Glioblastoma Multiforme

The most common primary brain tumours are gliomas, which originate from glial cells in the brain (Seliger & Hau, 2018). The World Health Organization (WHO) has classified gliomas from low (I-II) to high (III-IV) grade, based on aggressiveness and patient prognosis, with the most aggressive cancer, Glioblastoma Multiforme (GBM), classified as a grade IV glioma (Louis et al., 2016). GBM is very heterogeneous and demonstrates high genomic instability, making the recurrent tumour more aggressive and resistant to treatment. The average lifespan of GBM patients after diagnosis, under the standard of care, is 12-15 months (Zimmer et al., 2019). GBM patients undergo a very aggressive treatment regimen, beginning with maximal surgical resection, followed by radiotherapy and chemotherapy (Jia, Wang, Yin, & Liu, 2019). Chemotherapy almost always consists of temozolomide (TMZ), which may or may not be beneficial for patients, depending on the methylation status of MGMT, a gene known to inhibit the function of TMZ. This indicates a significant problem in current treatment options for GBM patients, as patients are still being treated with TMZ achieving complete response at a rate of only 11% (Gilbert et al., 2002).

2. Main Obstacles in GBM Treatment.

2.1. Cancer Stem Cells/Brain Tumour Initiating Cells

Cancer stem cells (CSCs) play an essential role in therapy resistance and tumour relapse in cancer (Brown et al., 2017). It is now known that CSCs represent a small subpopulation of cells within tumours and have stemness characteristics such as capacity to self-renew and generate differentiated cells that contribute to tumour heterogeneity

(Kreso & Dick, 2014). The first evidence of CSCs was in acute myeloid leukemia (AML), with the AML-initiating cells being identified based on the expression of a cell surface marker, the cluster of differentiation 34 ($CD34^+$), and the absence of the marker, cluster of differentiation 38 ($CD38^-$) (Lapidot et al., 1994). Different types of CSCs can be isolated in the lab based on their cell surface marker expression status, which includes $CD44^+/CD24^-$ (breast cancer) (Al-Hajj, Wicha, Benito-Hernandez, Morrison, & Clarke, 2003), $CD133^+/CD24^+/ESA^+$ (pancreas) (Li et al., 2007) and $CD133^+$, $CD44^+$ (glioma) (Hemmati et al., 2003; Singh et al., 2004).

Glioma CSCs are also referred to as brain tumour initiating cells (BTICs) and glioma stem cells (GSCs), and will be referred to as BTICs in this thesis. There is data to support that BTICs cause therapy resistance and tumour recurrence (Brown et al., 2017; Singh et al., 2004). They are often characterized by expression of proteins such as CD133, CD44, SOX2, and OCT4, to name a few (Bradshaw et al., 2016; Brown et al., 2017; Singh et al., 2004). CD44, a transmembrane glycoprotein involved in migration and invasion, and angiogenesis, is used by BTICs and contributes to aggressiveness of tumours (Senbanjo & Chellaiah, 2017). Spy1, also known as Speedy or RINGO, is a non-cyclin cell cycle regulator protein which is also found to be highly expressed in GBM (Ferby, Blazquez, Palmer, Eritja, & Nebreda, 1999; Lenormand, Dellinger, Knudsen, Subramani, & Donoghue, 1999; Lubanska et al., 2014). Spy1 binds to and activates cyclin-dependent kinase 2 (CDK2) independent of cyclin binding, allowing for a premature G_1/S phase transition in the cell cycle. Spy1 also promotes cell survival in response to DNA damage caused by genotoxic agents (Barnes, Porter, Lenormand, Dellinger, & Donoghue, 2003; Porter et al., 2002). Spy1 protein levels are upregulated in

increasing stages of glioma, with grade III glioma and GBM having the highest levels. Lubanska et al. showed that Spy1 advances the expansion of $CD133^+$ BTIC populations, possibly through the Numb/Notch pathway, making Spy1 a valid marker for BTIC expansion (Lubanska et al., 2014).

Current chemotherapies largely target cancer cells based on their high proliferation, affecting the rapidly dividing cells of the tumour. However, BTICs, like CSCs found in other tissues, have a slower rate of division and thus mediate chemoresistance and tumour recurrence following treatment (Baumann, Krause, & Hill, 2008; Eyler & Rich, 2008). There are other mechanisms contributing to the chemoresistance of BTICs, which include the expression of ATP-binding cassette (ABC) transporters. The ABC transporter proteins are a superfamily of membrane proteins capable of converting energy from ATP hydrolysis to transport various substrates across the cell membrane (Begicevic & Falasca, 2017). The ABC transporters C1 and B1 are both highly expressed in BTICs and act to actively efflux many drugs, including TMZ, etoposide, doxorubicin, and paclitaxel, among many others (Kolenda et al., 2011; Xi et al., 2016). Hence ABC transporters contribute to the chemoresistance in BTICs that make treating GBM particularly challenging. Another factor contributing to the drug resistance in BTICs is the ability of these cells to activate the DNA damage response and repair machinery (Maugeri-Sacca, Bartucci, & De Maria, 2012). BTICs can activate the ataxia-telangiectasia-mutated (ATM) serine/threonine kinase as well as the DNA damage checkpoint kinases 1 (Chk1) and 2 (Chk2) in response to ionizing radiation, allowing the BTICs to stall the cell cycle and repair DNA to avoid apoptosis (Bao et al., 2006). In summary, BTICs contribute to the resistance of therapy and tumour relapse in GBM

patients, and it is important to find drugs or treatment methods that target this population of cells to improve the prognosis in GBM patients.

2.2. The Blood-Brain Barrier

A major issue in treating most central nervous system (CNS) diseases, including brain cancers, is the ability to readily cross the blood-brain barrier (BBB). The BBB is a semipermeable membrane that separates the brain from the circulating blood supply. Consisting of different cell types such as cerebrovascular endothelial cells (CECs), pericytes, astrocytes, and microglial cells, the BBB is a complex network of cells providing an essential function to all vertebrates (Bundgaard & Abbott, 2008; Wang et al., 2018). The CECs form tight junctions between cells and are usually the prominent barrier in preventing molecules from crossing into the brain fluid (Wang et al., 2018). The BBB allows for the passage of some molecules by passive diffusion, and other critical molecules for proper neural function via selective transport, such as water, amino acids, and glucose (Groothuis, 2000; Liebner, Czupalla, & Wolburg, 2011). The BBB is an essential protective barrier to the most sensitive organ in the body; it is responsible for limiting pathogens, solutes in blood, and large or hydrophilic molecules from entering the cerebrospinal fluid (CSF). Although it does allow the diffusion of small hydrophobic molecules such as O_2 and CO_2, as well as small polar molecules, such as acetaminophen, the BBB is a major obstacle in the treatment of most CNS diseases, including brain cancer, by limiting the access of therapeutic drugs to cross into the CSF (Johansen et al., 2018; Stamatovic, Keep, & Andjelkovic, 2008). This also poses an obstacle in testing of new drug targets at the clinical level and impairing any progress in therapy. There are two major factors contributing to BBB penetration, the drug size must be lower than 400-500

Da, and the drug must form less than 8-10 hydrogen bonds with water (Cardoso, Brites, & Brito, 2010; Pardridge, 2005). These criteria can be used as a general rule when developing new drugs for treatment of diseases within the CNS, but a clinical trial will verify the actual amount of drug that effectively crosses the BBB. Unfortunately, current approach to drug development is focused on the target effect, and less effort is spent on the delivery of the drug (Pardridge, 2009). One method to get around the BBB in the treatment of GBM is through the use of a Gliadel® wafer. Carmustine, also known as BCNU, is infused in the Gliadel® wafer, which is implanted under the skull in the space left after the surgery to remove the GBM tumour. The wafer slowly dissolves, releasing the drug into the space left after surgery (Xing, Shao, Qi, Yang, & Wang, 2015). Although carmustine can readily cross the BBB, it has fewer toxic effects when used in a wafer. This method allows for other large molecules to be applied directly to the former tumour site. The Gliadel® wafer improves survival rates, but the drug delivery over time is short and not ideal, as the majority of drug is released in the first week (Domb et al., 1995; Shapira-Furman et al., 2019). The ideal wafer would release a consistent amount of drug over a longer time period. This method illustrates one way to treat GBM without having to consider the BBB. Another method of getting around the BBB is through the use of pulsed ultrasound with injected microbubbles – microscopic bubbles of an innocuous gas surrounded in a lipid coating – direct into the bloodstream. These microbubbles will vibrate and disrupt the BBB when ultrasound is applied, and this vibration disrupts the BBB and allows for drug passage that would not occur with an intact BBB (Carpentier et al., 2016). Disruption of the BBB is a new and experimental treatment method that requires more research and optimization.

3. The Cell Cycle and Cancer

The cell cycle consists of four separate phases, with checkpoints in-between and within phases. The first growth phase, called Gap 1 phase (G_1), is where cells gather enough nutrients to duplicate their DNA. The second phase is S phase, or synthesis phase, where DNA is synthesized. The third phase is the Gap 2 phase (G_2), where more nutrients are taken up and the cell prepares for the last phase, mitosis or M phase, where the cell undergoes mitosis and divides into two daughter cells. Cells have the capacity to enter a non-growth phase, G_0, before it commits to replicating DNA. Most non-dividing, non-growing cells in the human body, such as neurons and myocytes, are resting in the G_0 phase (Norbury & Nurse, 1992). There are also four well characterized checkpoints in the cell cycle, the first being located at the end of the G_1 phase, which checks for DNA damage, growth factors, and cell size. The next checkpoint is in the S phase, where there is continual control of DNA quality as DNA is being replicated. There is a checkpoint at the transition of the G_2 to M phase, which is similar to the checkpoint at the end of the G_1 phase, checking for DNA damage, sufficient nutrients and proper cell size to complete M phase. The last checkpoint is during M phase at the beginning of anaphase, called the spindle assembly checkpoint, which checks that chromosomes are aligned, and centromeres are properly attached to the microtubules for equal distribution. The checkpoints in the cell cycle are critical in maintaining healthy cells, by stopping the cell cycle after damage, the cell can repair the damage or follow apoptosis and eliminate any potentially harmful mutations (Kastan & Bartek, 2004).

The two major protein classes regulating the cell cycle are cyclins and CDKs. There are as many as 29 different cyclins and 20 different CDKs in humans as of this

writing, but the major cyclins involved in cell cycle regulation include cyclins A, B, D, and E. Not all cyclins or CDKs are involved in cell cycle regulation, but the major CDKs which are involved include CDKs 1, 2, 4, and 6 (Li, Qian, & Sun, 2019; Shen, Dean, Yu, & Duan, 2019; Vermeulen, Van Bockstaele, & Berneman, 2003).

CDKs consist of a family of serine/threonine protein kinases, which are constitutively expressed in cells, whereas specific cyclins are synthesized at specific points in the cell cycle, hence their namesake. CDKs form a complex with cyclins, and most CDKs have both activating and inhibitory phosphorylation sites that cause conformational changes which may allow the complex to form and become activated (Lim & Kaldis, 2013; Vermeulen, Van Bockstaele, & Berneman, 2003). These complexes push the cell through the checkpoints in-between the phases in the cell cycle. To be more specific, it is the binding of CDK4 and CDK6 to the group of cyclin D (cyclin D1, cyclin D2, and cyclin D3), and the downstream phosphorylation events from this complex, which are responsible for entry into the early G_1 phase (Sherr, 1994). Cyclin E-CDK2 complex is responsible for promoting the transition from G_1 to S phase (Ohtsubo, Theodoras, Schumacher, Roberts, & Pagano, 1995); CDK2 also binds with cyclin A and this complex is required for transition through S phase (Girard, Strausfeld, Fernandez, & Lamb, 1991; Walker & Maller, 1991). Cyclin A-CDK1 complex promotes the cell into the M phase, and the cyclin B1-CDK1 complex is also responsible for regulation in mitosis (Arellano & Moreno, 1997).

CDK activity is also regulated by another protein family, called CDK inhibitors (CKIs), which consist of two major groups; the INK4 family, which bind to CDK 4/6 proteins, and the CIP/KIP family, which bind to both CDK and cyclin together in

complex (Carnero & Hannon, 1998; Hengst & Reed, 1998). The INK4 proteins consist of $p15^{INK4b}$, $p16^{INK4a}$, $p18^{INK4c}$, and $p19^{INK4d}$, which inhibit CDKs 4 and 6 by forming stable complexes with CDK enzyme before binding with cyclin D, and thus block progression of the cell cycle past the G_1 checkpoint (Kim & Sharpless, 2006; Ortega, Malumbres, & Barbacid, 2002). INK4 proteins are tumour suppressor proteins that play a role in apoptosis, DNA repair, and senescence (Canepa et al., 2007; Roussel, 1999). The three proteins of the CIP/KIP family include $p21^{cip1/waf1}$, $p27^{kip1}$, and $p57^{kip2}$ (Harper et al., 1995; Lee, Reynisdottir, & Massague, 1995; Polyak et al., 1994), and their main action is inhibiting the G_1/S and S phase CDKs (CDK1 and CDK2) (Sherr & Roberts, 1999). Unlike the INK4 family, the CIP/KIP proteins have CDK independent roles in the cell, which include the regulation of transcription, apoptosis, and the cytoskeleton (Besson, Gurian-West, Schmidt, Hall, & Roberts, 2004; Coqueret, 2003; Wang, Elson, & Leder, 1997). The CIP/KIP family of proteins are responsible for inhibiting the cell cycle in the G_1 phase, inhibiting mostly the CDK2/4-cyclin complexes (Roskoski, 2019).

The cell cycle has many connections to the hallmarks of cancer (Hanahan & Weinberg, 2011). Mutations causing the inactivation of CKIs such as in p16, p21, and p27, remove the checkpoints in the cell cycle, allowing the cell to progress and divide. This allows for uncontrolled cell growth and evasion of apoptosis, as well as genomic instability, which contributes to tumour evolution (Hanahan & Weinberg, 2011; Williams & Stoeber, 2012). The CDKs involved directly in regulating the cell cycle are upregulated and often have increased activity in many cancers (Otto & Sicinski, 2017). Inhibition of CDK2 in BTICs causes a downregulation of Sox2 levels, which is involved in pluripotency (Liu et al., 2017). It is also common that GBM patients have

amplifications of CDK 4 and 6, as well as deletions or inactivating mutations of *CDKN2A*, which codes for p16 and p14, responsible for inhibiting CDK4 and CDK6 (Bronner et al., 2019). Other members of the CDK family are also involved in cancer, which include CDK5, which promotes invasion and migration by down regulating the actin regulatory protein caldesmon (Cheung & Ip, 2012; Quintavalle, Elia, Price, Heynen-Genel, & Courtneidge, 2011), CDK8 has been identified as a coactivator of the β-catenin pathway in colon cancer (Firestein et al., 2008), and CDK10 causes resistance to endocrine therapy in breast cancer (Iorns et al., 2008).

4. Common CNS Chemotherapies and Synthetic CKIs

4.1. Standard of Care and Other Chemotherapy

Currently the two most commonly used chemotherapy drugs for GBM treatment are TMZ and carmustine (Minniti, Muni, Lanzetta, Marchetti, & Enrici, 2009; Rahman et al., 2014). TMZ acts by alkylating/methylating DNA, at the N-7 or O-6 position of guanine (Zhang, Stevens, & Bradshaw, 2012). This DNA damage signals the cell for apoptosis, making it a useful chemotherapy. The action of TMZ can be counteracted by the DNA repair gene *MGMT*, an enzyme capable of repairing the mutagenic lesion of O6-methylguanine. The methylation status of the promoter of *MGMT* is a very powerful prognostic marker in GBM. The methylated *MGMT* promoter results in the repression of the MGMT protein, and therefore repression in DNA repair allowing for successful action of TMZ (Wang et al., 2019). In 2004, a study by Hegi et al. showed that patients with methylated *MGMT* promoter and treated with radiotherapy and TMZ had a median survival of 21.7 months, compared to 15.3 months in patients treated with only radiotherapy. In patients with an unmethylated *MGMT* promoter status, and thus an

increased amount of the MGMT repair protein, the comparable survival rates were 12.7 and 11.8 months, respectively (Hegi et al., 2005). Unfortunately, the standard of care in GBM treatment includes TMZ, regardless of *MGMT* methylation status.

TMZ or its derivatives can be delivered to a patient either intravenously or orally and can be administered in combination with various treatment regimens. The current standard treatment regimen is daily oral administration of 150-200 mg/m^2 for 5 days over a 28-day treatment cycle for 6 cycles following radiotherapy (Gilbert et al., 2013). TMZ requires first-pass metabolism to be activated, making it a prodrug, which is a compound that is pharmacologically activated after it has been administered and metabolized. At physiological pH, TMZ is metabolized into 3-methyl-(triazen-1-yl) imidazole-4-carboxamide (MTIC), which splits into two other metabolites responsible for methylating DNA (Agarwala & Kirkwood, 2000). The second most used drug in GBM treatment is carmustine, which is used in Gliadel® wafers inserted directly into the brain at the time of surgery. Carmustine is an alkylating agent that can cause the formation of interstrand crosslinks in DNA (Weiss & Issell, 1982; Woolley, Dion, Kohn, & Bono, 1976). Another drug which is used to treat GBM, among other cancers, is Etoposide, a topoisomerase II inhibitor (Tonder, Weller, Eisele, & Roth, 2014). It forms a stable complex with DNA and topoisomerase II, which prevents re-ligation and leads to double strand breaks in the DNA (Chen, Chan, & Hsieh, 2013; Wilstermann et al., 2007; Wu et al., 2011). This leads to a stop largely at the G_2/M checkpoint in the cell cycle (Higginbottom, Cummings, Newland, & Allen, 2002; Nam, Doi, & Nakayama, 2010). These drugs represent the conventional chemotherapy approach, non-specifically targeting rapidly growing cells and leaving behind the CSCs, permitting tumour relapse.

4.2. Synthetic CKIs

Natural CKIs are frequently mutated or deleted in cancer, allowing for unregulated cell proliferation (Bailon-Moscoso, Cevallos-Solorzano, Romero-Benavides, & Orellana, 2017; Johansson & Persson, 2008; Sharma, Sharma, & Tyagi, 2008). Since the downregulation of natural CKIs contributes to cancer progression, generation of synthetic CKIs has the potential to aid in eradication of therapy resistant cancer cells. The first synthetic CKI identified was flavopiridol in 1992, a pan-CDK inhibitor that inhibits CDKs 1, 2, 4, 6 and 7 (Kaur et al., 1992; Sedlacek, 2001). Since then there have been many synthetic CKIs developed and tested against cancer and a host of other diseases. The first FDA approved CKI, palbociclib, an inhibitor of CDKs 4 and 6, was approved for use in metastatic estrogen receptor positive breast cancer in combination with letrozole in 2015 (Morikawa & Henry, 2015), and there are now two other FDA approved CKIs as of this writing, abemaciclib and ribociclib (Kim, 2017; Mullard, 2017).

There are currently many clinical trials involving CKIs as single agent use or in combination with other chemotherapies. One such CKI is dinaciclib, a potent second generation CKI which targets CDKs 1, 2, 5, and 9 (Parry et al., 2010). Dinaciclib is currently in phase I and II clinical trials with one completed phase III trial. One study found dinaciclib, in combination with Bcl-2/Bcl-xL inhibitors, significantly reduced GBM cell proliferation independent of p53 status (Jane et al., 2016). Dinaciclib binds to the ATP site of CDK2 with an intricate network of hydrogen bonds and van der Waals forces, which explains its high potency and selectivity for CDK2 (Martin, Olesen, Georg, & Schonbrunn, 2013). Dinaciclib thus has great potential for treatment of GBM, as several oncogenes cause synthetic lethality with CDK2 inhibition (Cheng et al., 2012;

Lubanska & Porter, 2017; Molenaar et al., 2009). As a relatively new and understudied drug, there is little known about dinaciclib, including any first pass effects or whether it would be a good candidate drug used to cross the BBB. Clinical trials involving dinaciclib have included cancers such as leukemia, melanoma, non-small-cell lung cancer, and prostate cancer, but there are no trials involving GBM or any other brain cancers (Nemunaitis et al., 2013; Rello-Varona et al., 2019). Due to its potency *in vitro* and promising number of clinical trials for other types of cancer, it is of high importance to test the effectiveness of this compound against BTICs.

O6-cyclohexylmethylguanine, referred to hereafter as NU2058, is an inhibitor of CDK2 and CDK1, with K_i values of 12 ± 3 and 5 ± 1 μM, respectively. The K_i is defined as the inhibitory constant and is reflective of the binding affinity of compounds. NU2058 binds to the ATP binding pocket of CDK2, in a distinct position which differs from other purine-based inhibitors, such as roscovotine (Arris et al., 2000; Hardcastle et al., 2004; Rigas, Robson, & Curtin, 2007). The pharmacology of CKIs such as first-pass metabolism and half-life are lacking, and the field requires further research.

4.3. Drug Interactions and Bliss Independence Model

Drug interactions are an important aspect of every anti-cancer regimen due to their ability to either diminish or enhance the action of an individual drug in the applied combination. Drug interactions can be additive in effect, which is the expected result when the drugs have no interactions; synergistic, the effect of interacting drugs is larger than the expected additive result; and antagonistic, the reduced outcome from the expected additive results (Greco, Bravo, & Parsons, 1995). The use of a drug as a monotherapy has its limits and downfalls, as chemotherapies used alone typically only have one target, the efficacy is

inadequate and the heterogenous tumour typically relapses from the resistant CSCs (Spiro, Kovacs, & Csermely, 2008). Synergy between drugs is very important in treating cancer. When two or more drugs are used, synergistic effects are desirable because of increased efficacy and the decreased dosage used with the same or greater than expected efficacy as opposed to the drugs used alone. The decreased dosage of synergistic drugs causes fewer toxic effects seen in patients, and in general, drugs used in combination delay the progress of drug resistance (Jia et al., 2009).

There are a few common methods used to calculate the drug interactions, which include the Bliss independence model, Loewe additivity, and the Chou-Talalay method (Bliss, 1939; Chou & Talalay, 1977; Loewe, 1928). These models are important in determining which drugs can be used synergistically against cancer. These methods used to calculate drug interactions address the same question but from different viewpoints. Conceptually, the Bliss independence model emphasizes the treatment effect enhancement, while the Loewe additivity model emphasizes on dose reduction, making the Bliss independence model a more suitable model to study chemotherapy drug combinations (Lotsch & Geisslinger, 2011; Zhao et al., 2014). The Bliss independence model assumes no interaction between drugs and the combined drugs have different mechanisms of action or target sites from each other (Foucquier & Guedj, 2015; Pemovska, Bigenzahn, & Superti-Furga, 2018).

5. Zebrafish as a High-Throughput *in vivo* Model

Animal models play an essential role in the development of novel anti-cancer drugs. Mice have been established as the golden standard for model organisms when investigating cancer biology under new therapy testing, which is due to the high genetic similarities

between humans and mice, amongst many other reasons (Lampreht Tratar, Horvat, & Cemazar, 2018). Despite multiple advantages of employing mice, mouse models are relatively expensive and labour intensive, diminishing their utility in high-throughput drug screening studies. Zebrafish (*Danio rerio*) have been established as an animal model for developmental genetics in the 1960's (Streisinger, Walker, Dower, Knauber, & Singer, 1981). Approximately 70% of protein coding genes in zebrafish have their human orthologs (Howe et al., 2013), and zebrafish do have similar physiology to humans, which include organs such as heart, liver, and pancreas. These organs perform much of the same functions as their human counterparts, such as the BBB, which is functionally conserved in zebrafish and contain proteins responsible for tight junctions in the human BBB, such as claudin-5 and ZO-1 (Fleming, Diekmann, & Goldsmith, 2013; O'Brown, Pfau, & Gu, 2018). Another example is the cardiac electrophysiology, which in zebrafish is more similar to humans than humans are to mice, with a comparable electrocardiogram (ECG) between humans and zebrafish (Asnani & Peterson, 2014; Chi et al., 2008; MacRae & Peterson, 2015). Additionally, cytochrome P450 is a family of enzymes responsible for oxidation of endogenous and exogenous chemicals. In humans, these enzymes are responsible for about 75% of drug metabolism. Zebrafish have a total of 94 cytochrome P450 genes, most of which are direct orthologs of human cytochrome P450 (Goldstone et al., 2010). A representative image of a zebrafish embryo aged 4 days post fertilization (4dpf) and its anatomy are presented in Figure 1A.

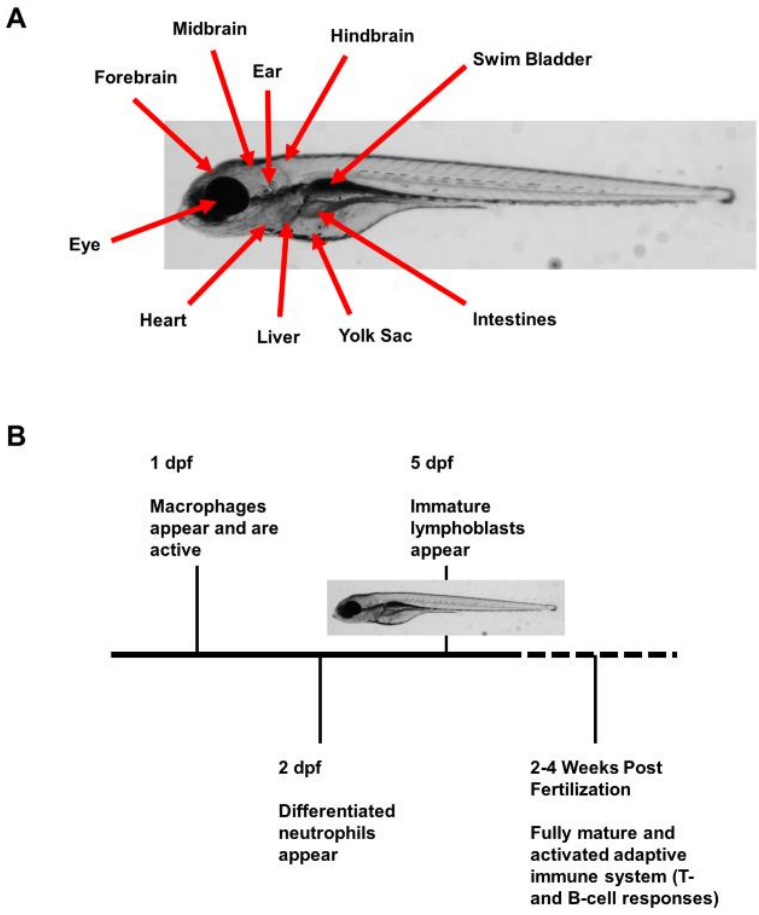

Figure 1: Anatomy and immune development of the zebrafish embryo.

(A) Image of a zebrafish embryo aged 4dpf with labelled anatomy. (B) Simplified timeline of the immune system development in zebrafish. Note the adaptive immune system (T- and B-cells) are not active until 2-4 weeks post fertilization. Image of zebrafish embryo taken and provided by Janice Tubman.

Furthermore, zebrafish have become an efficient tumour xenotransplantation model first described by Lee et al. in 2005, who transplanted melanoma cells into the blastodisc of very young (3.5 hours post fertilization) zebrafish embryos, promoting the idea of zebrafish for tumour-based experiments (Lee, Seftor, Bonde, Cornell, & Hendrix, 2005). There are many advantages for the use of zebrafish as an animal model in tumour xenotransplantation studies in comparison to mice. One advantage is the rapid embryonic development, giving researchers eggs in less than 24 hours to work with. Compared to mice with a gestation period of 21 days, zebrafish allow for faster experiments. Zebrafish prefer to be housed in large groups, called shoals, and are much smaller requiring far less maintenance than mice (Streisinger, Walker, Dower, Knauber, & Singer, 1981). Zebrafish also produce many more spawn than mice, producing around 100-200 eggs per breeding pair, compared to an average of 7-12 pups per litter in mice (Lampreht Tratar, Horvat, & Cemazar, 2018; Mullins, Hammerschmidt, Haffter, & Nusslein-Volhard, 1994; Streisinger, Walker, Dower, Knauber, & Singer, 1981). The development of the immune system in zebrafish (Figure 1B) plays a critical role for the use of zebrafish in cancer research. The adaptive immune system of the zebrafish is not fully active until fish are around 21 days old, and there is an immature innate immune response starting at 24 hours post fertilization (hpf). This allows for a primitive immune response against bacterium, but injected cells are not detected by this innate immune system, allowing for tumour transplantation at an early developmental stage without the need for genetically altered immunocompromised organisms (Lam, Chua, Gong, Lam, & Sin, 2004; Lieschke & Trede, 2009; Meijer & Spaink, 2011; Traver et al., 2003). Cells undergoing transplantation are typically labelled with fluorescent dyes or are altered to constitutively

express fluorescent protein in the cytoplasm, and then injected into the zebrafish, commonly into the yolk sac of the developing embryo but can also be injected orthotopically (the transplantation of specific tissue into its normal place in the body) and as a xenograft in immunocompromised adult fish (Wertman, Veinotte, Dellaire, & Berman, 2016). Because the embryos are transparent (Figure 1A), real-time live imaging in zebrafish is relatively easy, and transparent adult zebrafish lines have been developed allowing for live imaging at the single cell level, something not easily achieved in mice (Ghotra et al., 2012; Spitsbergen, 2007; Stoletov, Montel, Lester, Gonias, & Klemke, 2007; White et al., 2008; Zhao, Tang, Cui, Ang, & Wong, 2009).

Recent work has suggested that zebrafish can be a great model for the development of patient-personalized care, as patient-derived cells can be successfully xenografted into adult immunocompromised fish and treated with different drug combinations by orally gavaging fish (Yan et al., 2019). Zebrafish have been established as a model organism for drug screening because they produce many progenies per breeding pair, and there is enough fish that can be used to statistically evaluate the outcomes. This is typically done in multi-well plates and embryos can be placed in groups per well or individually in a single well. By performing drug screens this way, many drugs, as well as many drug combinations, can be tested at the same time (Gibert, Trengove, & Ward, 2013; MacRae & Peterson, 2015). All the advantages listed above contribute to the cost effectiveness of zebrafish, adding yet another advantage of zebrafish as an animal model for human cancer.

6. Hypothesis and Objectives

Hypothesis: Synthetic CKIs in combination with chemotherapy play an important role in treatment of glioma cells and demonstrate characteristics advantageous for potential combination therapy for patients with GBM.

Objectives: The first objective is to assess the effectiveness of a CKI and chemotherapy as a combination therapy on GBM *in vitro*. The second objective is to characterize the GBM cell populations post-treatment. Finally, the last objective is to assess the effectiveness of dinaciclib *in vivo* using the zebrafish animal model.

MATERIALS AND METHODS

1. Cell Culture

U-87 MG wild-type (WT) cells were obtained from ATCC and maintained in growth media containing Eagle's minimum essential medium (EMEM) (Quality Biological, #112-018-101) supplemented with 10% fetal bovine serum (FBS) (Gibco, #10437028) and 1% penicillin and streptomycin (Invitrogen, #15140148). Once cells reached 70-80% confluency, plates were washed with serum-free EMEM and 700µL of 0.25% trypsin (Hyclone, #SH3023601) was added and plate was incubated at 37°C for 3-5 minutes. Cells were cultured at 37°C in 5% CO_2 environment.

U-251 MG WT cells were a kind gift from Dr. Rutka (SickKids Hospital, Toronto) maintained in EMEM growth media supplemented with 10% FBS, 1mM sodium pyruvate, 1% non-essential amino acids, and 1% penicillin and streptomycin. Once cells reached 80-90% confluency, plates were washed with serum-free EMEM and 700 µL of 0.25% trypsin was added and plate was incubated at 37°C for 5 minutes. Cells were cultured at 37°C in 5% CO_2 environment.

MDA-MB-231 (HTB26; ATCC) cells were cultured in Dulbecco's Modified Eagle's Medium (DMEM; Sigma) supplemented with 10% FBS and 1% penicillin and streptomycin and were maintained in an atmosphere of 5% CO_2 at 37˚C.

2. MTT Assay and Bliss Independence Model

Cell viability was determined using an MTT (Thiazolyl Blue Tetrazolium Bromide) assay. Cells were seeded in a 96-well plate at a density of $5x10^3$ cells/well in a total of 100µL growth media, 24 hours before drug treatment began. The growth media was then replaced with fresh growth medium containing different concentrations of each of the

drugs TMZ (Selleckchem, #S1237), etoposide (Santa Cruz, #sc-3512), NU2058 (Santa Cruz, #sc-202744A), and dinaciclib (Selleckchem, #S2768) every 24 hours for 3 consecutive days. After 24 hours of the last drug treatment, growth media was removed and 100µL of a 50% mix of MTT solution (5mg/mL Thiazolyl Blue Tetrazolium Bromide in filter sterilized PBS) (Sigma Aldrich, #M5655) and serum-free EMEM media was added to the wells. The plate was then immediately incubated at 37°C for 3 hours, then 150 µL of MTT solvent (4 mM HCl, 0.1% NP40 in isopropanol) was added to each well and left on an orbital shaker for 15 minutes. Within one hour, plate was read on a SpectraMax plate reader (Molecular Devices) for absorbance at OD=590 nm. The EC_{50} values were calculated using the free software Combenefit (Di Veroli et al., 2016). EC_{50} is defined as the half maximal effective concentration, and the quantal dose response curve was calculated, which is the concentration of a compound where 50% of the population exhibit a response.

The Bliss independence model was used for analysis of all combination drug treatments. The Combenefit software (Di Veroli et al., 2016) was used to determine the drug interactions using the Bliss model. The Bliss equation is as follows:

$$Y_{ab,P} = Y_a + Y_b - Y_a Y_b$$

Where $Y_{ab,P}$ is the predicted percent inhibition, Y_a is percent of inhibition from drug *A* at dose *a*, and Y_b is the percent of inhibition from drug *B* at dose *b*. Then the observed percentage inhibition is calculated in the same way, denoted as $Y_{ab,O}$, which is then compared to the $Y_{ab,P}$ value. If $Y_{ab,O} = Y_{ab,P}$ then there is an additive effect, if $Y_{ab,O} > Y_{ab,P}$ then there is a synergistic relationship of the two drugs in question, and if $Y_{ab,O} <$

$Y_{ab,P}$ then there is an antagonistic relationship of the two drugs in question (Zhao et al., 2014).

3. Immunocytochemistry

Cells were grown on coverslips in 6-well plates at 37°C and 5% CO_2. Growth medium was aspirated off adherent cells and washed with warmed PBS twice. Cells were then fixed with 1 mL of 4% paraformaldehyde (PFA) for 15 minutes, then 800 µL were removed and 800 µL of PBS was added to each well. Plates were then wrapped in parafilm and stored at -20°C until ready for continuation. Once ready, PFA/PBS mixture was removed, cells were washed again with PBS, and coverslips were moved onto labelled parafilm. Cells were washed 3 times with PBS-Triton Wash Buffer (0.05% Triton X-100 in PBS) for 5 minutes each time. Cells were then blocked with blocking buffer for 1 hour at room temperature. The primary antibodies CD44 (Novus, #NBP1-31488) (3.3:400), Ki67 (Abcam, #ab15580) (1:400), and CC-3 (cleaved caspase-3) (Cell signalling, #9661S) (1:400) were prepared in 50% blocking buffer solution and 50% PBS-Triton wash buffer, and 100 µL drops were placed on parafilm per coverslip. Coverslips were placed cell side down onto primary antibody mixture and moved to a humidity chamber and incubated at 37°C for 1.5 hours. Afterwards, coverslips were moved onto parafilm at room temperature and washed 3 times with PBS-Triton wash buffer with 50% blocking buffer for 5 minutes each wash. Secondary antibody mixture was prepared in 50% blocking buffer in PBS-Triton wash buffer, and 100 µL drops were placed on fresh parafilm, coverslips placed cell side down onto drops, and moved to a humidity chamber at 37°C for 1 hour. Humidity chamber was covered with aluminum foil for light sensitive secondary antibody. Coverslips were removed from humidity

chamber and placed cell side up on parafilm at room temperature. Cells were then washed for 5 minutes in PBS, followed by a 5-minute wash in Hanks Balanced Salt Solution (HBSS). Then nuclear stain was done for 20 minutes at room temperature in Hoechst (3 mL Hoechst in 5 mL HBSS) and covered in aluminum foil. Cells were then washed with HBSS for 5 minutes, followed by PBS for 5 minutes, and then with distilled water for 5 minutes. Coverslips were then mounted to slides and stored for imaging. Images were taken using a Leica inverted microscope (Leica CTR 6500 microscope). Images were quantified using ImageJ.

4. Quantitative Real-Time Polymerase Chain Reaction (qRT-PCR)

RNA was extracted via Qiagen RNeasy Plus Mini Kit (Qiagen, #74136) as per manufacturer's instructions. Nanodrop lite Spectrophotometer (Thermofisher) was used to calculate concentration and purity of RNA elution. Synthesis of cDNA was done via qScript™ cDNA SuperMix Master Mix (Quantabio, #95048) as per manufacturer's instructions. cDNA was stored at -20°C for short term storage and -80°C for long term storage for future use. The qRT-PCR experiment utilized SYBR Green detection with Fast SYBR™ Green Master Mix (ThermoFisher, #A25780), and reactions were run for 40 cycles in 10 µL total. Analysis was completed using Viia7 Real-Time PCR System and software (Life Technologies). Samples were normalized to hGAPDH as an internal control. The primers used were as follows:

hGAPDH forward	5'-GCACCGTCAAGGCTGAGAAC-3'
hGAPDH reverse	5'-GGATCTCGTCCTGGAAGATG-3'
hSpy1 forward	5'-TTGTGAGGAGGTTATGGCCATT-3'
hSpy1 reverse	5'-GCAGCTGAACTTCATCTCTGTTGTAG-3'
hMAP2 forward	5'-AGGCTGTAGCAGTCCTGAAAGG-3'

hMAP2 reverse 5’-CTTCCTCCACTGTGACAGTCTG-3’

5. Animal Care and Toxicity Screen

WT zebrafish were handled in compliance with local animal care guidelines and standard protocols of Canada and following the animal utilization protocol #19-03. Adult zebrafish were kept at 28.5°C and bred according to “The Zebrafish Book” (Westerfield, 2000).

Eggs were collected and maintained in 28°C until 1dpf, where they were moved to 33°C and subsequent embryos were placed into 12-well plates at 8 embryos per well with E3 embryo media (5 mM NaCl, 0.17 mMKCl, 0.33 mM CaCl2, 0.33mM MgSO4, 10^{-5}% Methylene Blue). Starting at 3dpf, E3 media was replaced with E3 media containing either dinaciclib, NU2058, TMZ, or DMSO (dimethyl sulfoxide) at varying concentrations. Embryos were fed once at 4dpf, before new drug treatments began, for 30 minutes until media was changed and drugs were added. Media was changed daily for 3 consecutive days, before drug treatments began, and dead embryos were counted and removed each day. The sum of dead embryos was calculated 1 day after the last day of treatment (6dpf) and percentage of dead embryos was calculated.

6. Zebrafish Injections

Cells for zebrafish injections were fluorescently stained up to 2 hours before injection. Cells were washed with serum-free EMEM media and 0.25% trypsin was added for 5 minutes to allow adherent cells to detach from plate. A total of $5x10^5$ cells were collected and spun down at 1000 RPM for 5 minutes, media removed, and resuspended in 200 µL of serum-free media. Then 5 µL of Vybrant™ DiO (green) (Invitrogen) dye was added to cell suspension and incubated at 37 °C for 20 minutes, with a quick and gentle vortex every 5 minutes. Cells were spun down at 1000 RPM for 5 minutes at 4 °C, washed in

serum-free EMEM media, centrifuged again as above, and cells were resuspended in a final volume of 50 µL in serum-free EMEM media.

A 2% agarose gel was made in a 10 cm plate, and 0.168 mg/ml of Tricaine (Sigma, MS222) solution was prepared. A prepared needle was already pulled, and the day of injection was opened at the tip, placed into the Nanoject II microinjector (Drummond Scientific) and oil was taken up. Oil was then released partially, and cells were taken up into the needle. Embryos were anesthetized with tricaine before injection. Embryos were placed onto agarose gel and roughly 10 nL of cell suspension was injected into the yolk sac of embryos aged 2dpf. Successful injections were screened by imaging all injected fish next day with a Leica inverted microscope (Leica fluorescence stereomicroscope M205). Embryos were imaged at 35x magnification at the same exposure and intensity. Successfully injected embryos were separated and maintained in E3 media in 12-well plates at 8 embryos per well. Embryos were treated with dinaciclib or DMSO in E3 media daily for 3 days. Embryos were maintained at 28°C until 1dpf, and then moved to 33°C.

7. Zebrafish Imaging and Analysis

Embryos were imaged daily from 1 day post injection (1dpi) to 4dpi, and once at 7dpi. Embryos were anesthetized in tricaine and placed onto 2% agarose gel for imaging. A total of 4-5 embryos would be imaged at once, using a Leica fluorescent scope in the GFP channel. Images were imported into ImageJ, converted to 8-bit greyscale, and threshold was adjusted to eliminate background pixels. Threshold adjustments were kept the same for all images of all days. Labelled cells were measured as foci area under total area measured from raw integrated density. Results were moved to Excel, and total foci

area was normalized starting at the last day of treatment (3dpi), so each treatment group began with a normalized value of 1 on 3dpi.

8. Brain and Tail Metastasis Analysis

Images from 7dpi were used for analysis of metastases proximal to the brain. Foci were considered to be proximal to the brain if they were above/past the swim bladder towards the eyes, there was more than one foci away from the point of injection (yolk sac/intestines), and there was at least one foci in the area of the brain according to Figure 1B (forebrain, midbrain, hindbrain). Foci were considered to be metastases down the tail if they were past the swim bladder away from the eyes and there was more than one foci away from the point of injection (yolk sac/intestines). Images from 3dpi embryos of MDA-MB-231 injected cells were obtained from Janice Tubman. These images were analyzed under the same conditions for both brain and tail metastases.

9. Statistical Analysis

GraphPad Prism 8.0.2 software was used for all statistical analysis except for matrix plots of drug combinations. Drug combination and synergy evaluation significance was completed using the Combenefit (Di Veroli et al., 2016) software, a one-sample Student's t-test was performed to test significance of drug interaction. A one-way ANOVA was performed for number of nuclei, percent positive cells for antibodies Ki67, CD44, and CC-3 from Figure 5 B and C, and a Tukey's multiple comparison test was performed from 5 different field of views (FOV) for each treatment. A one-way ANOVA was performed on qRT-PCR data from Figure 5E with a Tukey's multiple comparison test from 3 separate experiments. Multiple t-tests using the Holm-Sidak method were performed on foci area in embryos from Figure 7B from 2 groups per treatment with a 6-

8 fish per group per treatment. A one-way ANOVA was performed on percentage of fish with metastases proximal to the brain with a Tukey's multiple comparison test from 2 groups with 6-15 fish per group per treatment. A two-way ANOVA was performed on the comparison of metastases down the tail and proximal to the brain between the U87 cell line and MDA-MB-231 cell line from 2 groups per treatment, with 16-29 fish per group.

RESULTS

1. Selected CKIs and Chemotherapeutics Have an Antagonistic Relationship

Combination therapy consisting of two or more therapeutic agents is a widely used approach in the clinic. To achieve the desired and successful treatment results, drugs are combined to complete, fine-tune, and even enhance the action of one another. To determine the potential synergistic relationship between CKIs and commonly used chemotherapies, the EC_{50} was first determined for each drug. The GBM cell lines U87 and U251 were used to determine the drug interactions of four different drugs, which include etoposide, TMZ, NU2058, and dinaciclib. EC_{50} values were determined using the cell viability MTT assay. All values and corresponding growth curves were calculated and produced using the free software, Combenefit (Di Veroli et al., 2016). Dinaciclib showed the strongest negative effect on cell viability and had the most consistent EC_{50} values between the U87 and U251 cell lines at 11.2 nM and 13.7 nM, respectively (Figure 2A).

Using Combenefit and the synergy and antagonism model, Bliss independence model, matrix plots of synergy distribution and matrix plots along with the corresponding surface plots of synergy distribution were developed for U87 cells (Figure 3) and U251 cells (Figure 4), respectively. The colour spectrum of the matrix plot presents antagonism increase, red marking high levels of antagonism, yellow marking slight antagonism, and green being an additive relationship. Alternatively, synergy increases as the colour spectrum moves from green to blue, darker blue being very synergistic and light blue being slightly synergistic. Values in the matrix plots represent the difference as a percentage from the control, with the control being the expected additive value of two

drugs, assuming there is no interaction between the two drugs. The results obtained for the U87 cell line show there was slight antagonism for most concentrations used between the drug combinations of NU2058 with etoposide and TMZ with dinaciclib (Figure 3). There was a marked increase in antagonism in the drug combination of etoposide with dinaciclib as dinaciclib concentration increased from 7.5 nM to 30 nM. The drug combination of NU2058 with TMZ showed mostly an additive effect of the two drugs in the different concentrations tested, however there was less significance within the matrix plot at each concentration combination. Data obtained for U251 cell line showed that every drug combination of a CKI with chemotherapy presented considerable antagonism (Figure 4). The values determined for the concentrations resulting in a more additive effect were found to be statistically not significant, unlike most antagonistic effects. Overall, the selected CKIs and chemotherapeutics used in combination had an antagonistic relationship in the U87 and U251 cell lines.

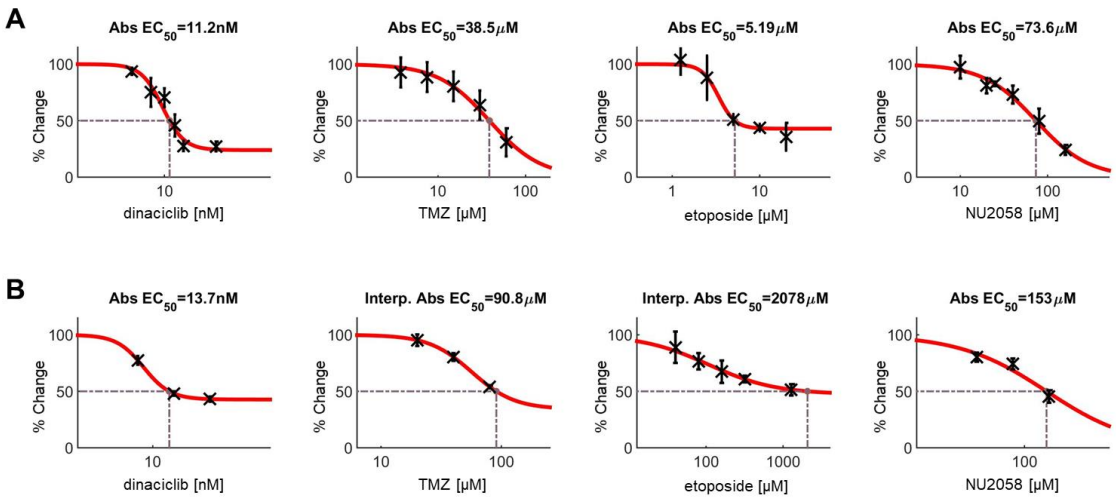

Figure 2: EC_{50} values and inhibition curves of GBM cell lines.

GBM cell lines were treated with either dinaciclib, TMZ, etoposide, or NU2058 daily for 3 days, and cell viability was calculated via MTT assay. All EC_{50} values and graphs were calculated with Combenefit software. (A) Represents U251 cell line and (B) represents U87 (U87-MG) cell line. Interpolated EC_{50} values were calculated for TMZ and etoposide in (B) due to low data points. All data points are given as a mean of 3 separate experiments, error bars represent standard error of the mean.

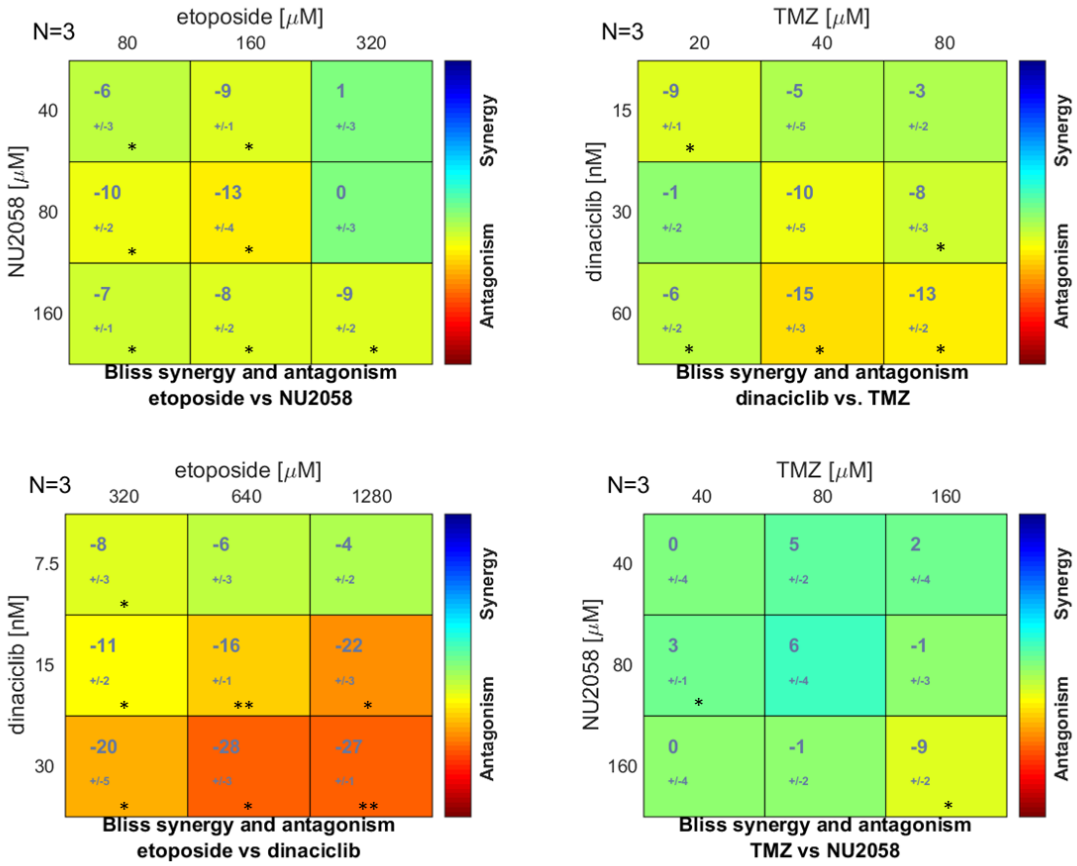

Figure 3: U87 matrix plots of synergy distribution from combination of a CKI and chemotherapy.

Matrix plots of synergy distribution from different drug combinations in the U87 cell line. Combinations included a CKI (dinaciclib or NU2058) and a chemotherapy (TMZ or etoposide). Cells were treated daily for 3 consecutive days. Values in each box of the matrix plot are given as an expected percentage difference from the additive effect of the 2 drugs combined, ranging from -100 (antagonism) to 100 (synergy). *p<0.05, **p<0.01. Statistical significance was determined by Combenefit Software using a one-sample t-test.

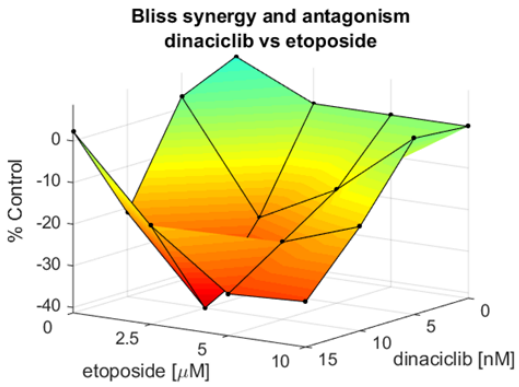
Bliss synergy and antagonism
dinaciclib vs etoposide
% Control
0
-10
-20
-30
-40
0
2.5
5
10
etoposide [μM]
0
5
10
15
dinaciclib [nM]

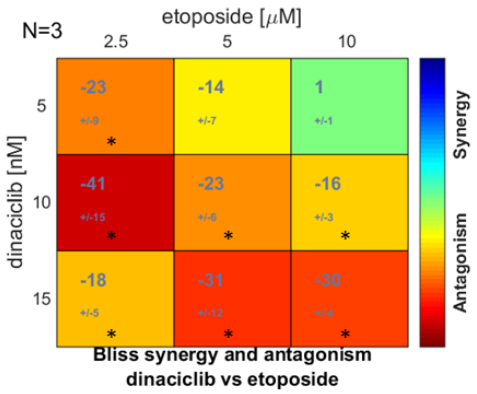
N=3
etoposide [μM]
2.5
5
10
dinaciclib [nM]
5
10
15
-23
+/-9
-14
+/-7
1
+/-1
-41
+/-15
-23
+/-6
-16
+/-3
-18
+/-5
-31
+/-12
-30
+/-4
Synergy
Antagonism
Bliss synergy and antagonism
dinaciclib vs etoposide

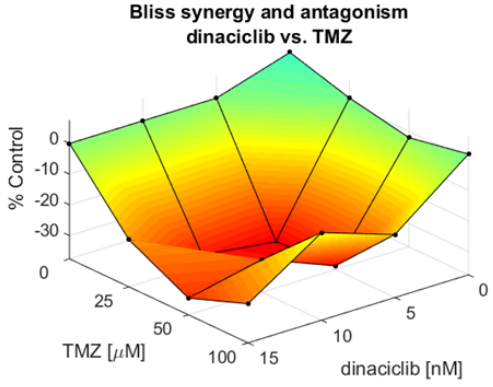
Bliss synergy and antagonism
dinaciclib vs. TMZ
% Control
0
-10
-20
-30
0
25
50
100
TMZ [μM]
0
5
10
15
dinaciclib [nM]

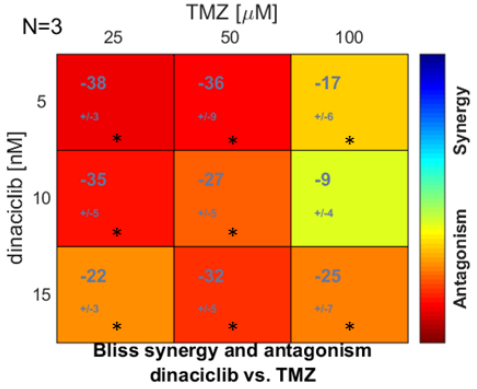
N=3
TMZ [μM]
25
50
100
dinaciclib [nM]
5
10
15
-38
+/-3
-36
+/-9
-17
+/-6
-35
+/-5
-27
+/-3
-9
+/-4
-22
+/-3
-32
+/-5
-25
+/-7
Synergy
Antagonism
Bliss synergy and antagonism
dinaciclib vs. TMZ

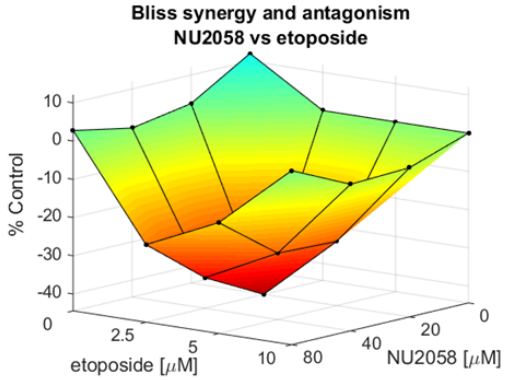
Bliss synergy and antagonism
NU2058 vs etoposide
% Control
10
0
-10
-20
-30
-40
0
2.5
5
10
etoposide [μM]
0
20
40
80
NU2058 [μM]

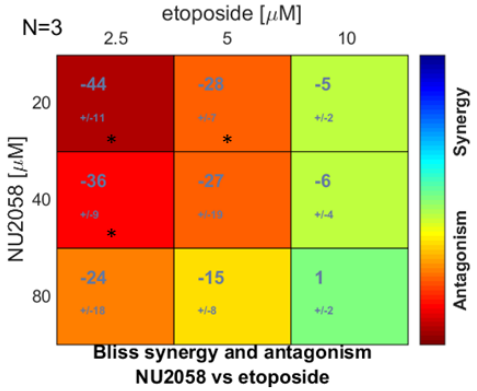
N=3
etoposide [μM]
2.5
5
10
NU2058 [μM]
20
40
80
-44
+/-11
-28
+/-7
-5
+/-2
-36
+/-9
-27
+/-13
-6
+/-4
-24
+/-13
-15
+/-8
1
+/-2
Synergy
Antagonism
Bliss synergy and antagonism
NU2058 vs etoposide

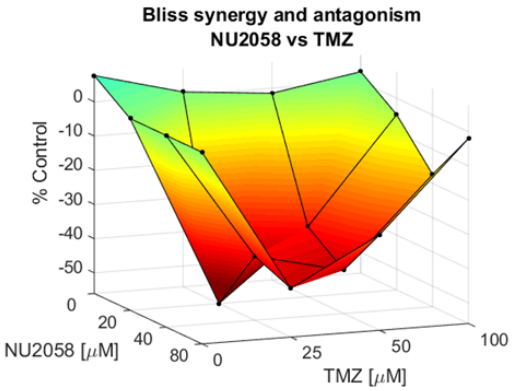
Bliss synergy and antagonism
NU2058 vs TMZ
% Control
0
-10
-20
-30
-40
-50
0
20
40
80
NU2058 [μM]
0
25
50
100
TMZ [μM]

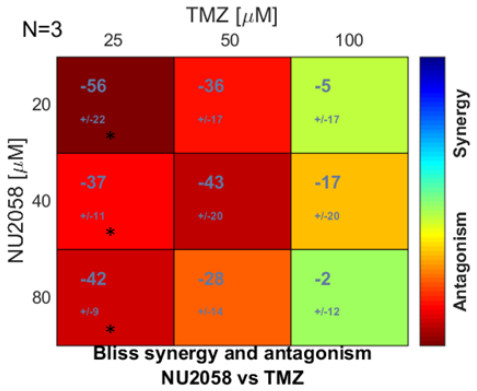
N=3
TMZ [μM]
25
50
100
NU2058 [μM]
20
40
80
-56
+/-22
-36
+/-17
-5
+/-17
-37
+/-11
-43
+/-20
-17
+/-20
-42
+/-9
-28
+/-14
-2
+/-12
Synergy
Antagonism
Bliss synergy and antagonism
NU2058 vs TMZ

Figure 4: U251 surface plots and the corresponding matrix plots of synergy distribution from combination of a CKI and chemotherapy.

Surface plots (left) and the corresponding matrix plots (right) of drug combinations used for U251 cell line. Cells were treated for 3 consecutive days. Values in each box of the matrix plot are given as an expected percentage difference from the additive effect of the 2 drugs combined, ranging from -100 (antagonism) to 100 (synergy). *$p<0.05$. Statistical significance was determined by Combenefit Software using a one-sample t-test.

2. Dinaciclib Selects for a Stem-like Population of GBM Cells

To analyze the post-treatment GBM cell populations, immunocytochemistry was performed utilizing U251 cells treated with dinaciclib, TMZ, or a combination of both. Cells were treated with 15 nM dinaciclib, or 50 μM TMZ, or a combination of both drugs. These values were slightly higher than the calculated EC_{50} values for U251 cells (11.2 nM for dinaciclib, 38.5 μM for TMZ). Cells were stained with antibodies for the proliferation marker Ki67, the stem-cell marker CD44, the apoptosis marker CC-3, and DAPI for nuclear staining. Slides were imaged (Figure 5A) and 5 images per slide were taken at the magnification of 20x and analyzed using ImageJ. Dinaciclib significantly decreased total number of nuclei per FOV, both as a single agent and in combination with TMZ, compared to the control, treated with an equivalent amount of DMSO, as well as to TMZ alone (Figure 5B). Next, the staining was quantified to determine the percent of positive cells for each antibody (Figure 5C). Dinaciclib significantly increased the number of cells positive for the proliferation marker Ki67 in the remaining post-treatment cell population, compared to control, and when used in combination with TMZ the proliferation marker was also significantly increased compared to the control and TMZ alone. A similar effect was observed for the stem cell marker CD44 expression. Dinaciclib significantly increased the amount of $CD44^+$ cells when used alone or in combination with TMZ compared to both TMZ alone and the control. There was a significant increase of roughly 20% of cells positively staining for CC-3 observed in the dinaciclib/TMZ combination treatment compared to control. Analysis of the GBM post-treatment populations suggests that dinaciclib is selecting for a more stem-like population.

To further characterize and confirm the stemness of the remaining population after dinaciclib and TMZ combination treatment, cells were treated with vehicle control, dinaciclib, TMZ, or the combination of both at the same concentrations and conditions as above. Cells were collected and a qRT-PCR was conducted (Figure 5D). Results are given as $\log_{10}$ RQ (relative quantity) in comparison to the control. Dinaciclib and the combination of dinaciclib and TMZ caused significant increases in the GBM cell clonal expansion marker, *SPDYA*, coding for Spy1 protein, compared to TMZ treatment alone. *MAP2* is a commonly used differentiation marker, responsible in cytoskeleton regulation in brain nerve cells. There is lower expression of *MAP2* in gliomas compared to normal brain tissue (Zhou et al., 2015). There was also a significant decrease in *MAP2* transcript levels of the combination treatment of dinaciclib and TMZ when compared to TMZ alone. Dinaciclib also caused a decrease in *MAP2* transcript levels when compared to the control group and TMZ alone, although these results are not statistically significant (Figure 5E). In summary, dinaciclib inhibits growth of GBM cells and selects for a more stem-like population.

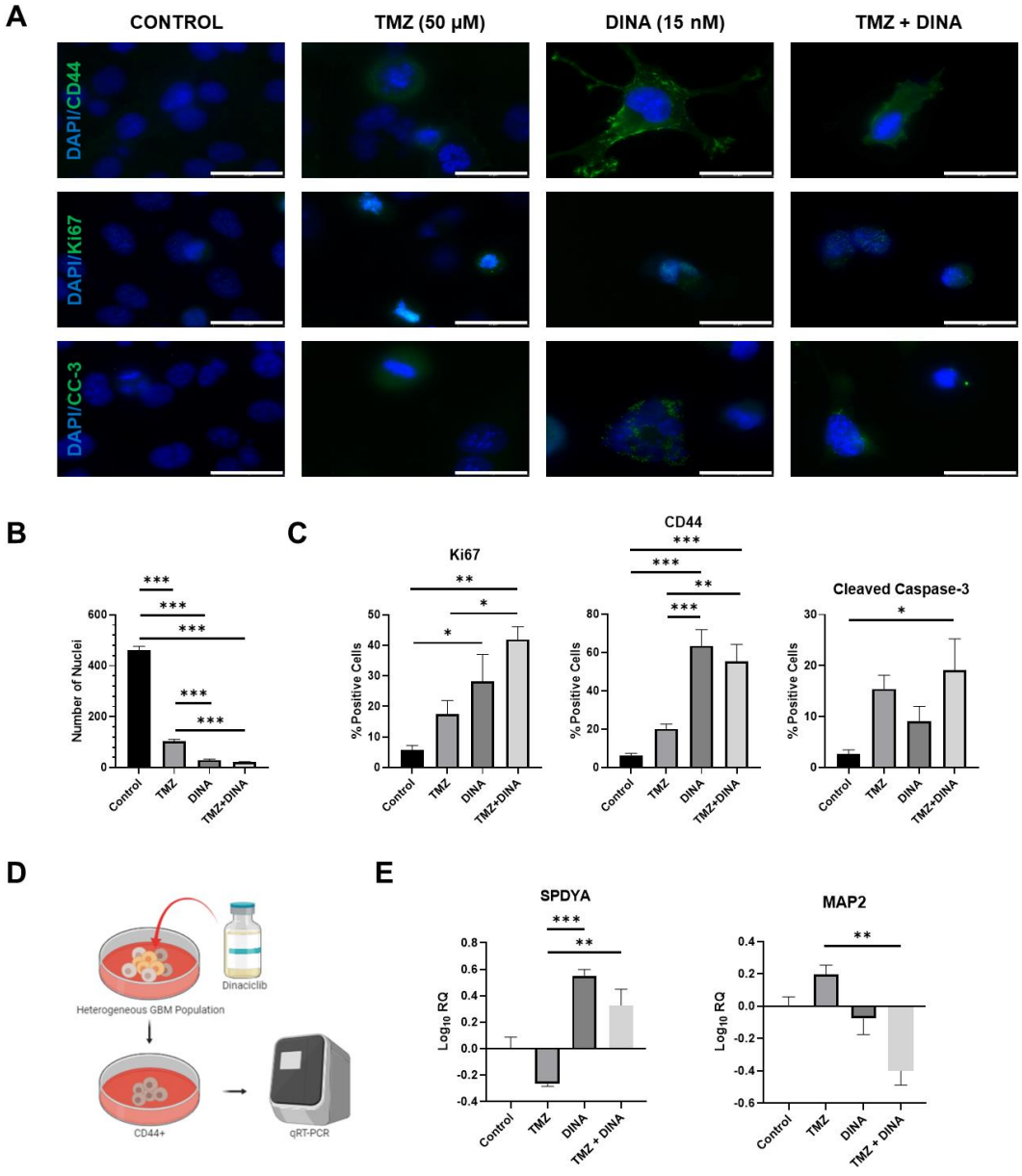
A
CONTROL
TMZ (50 μM)
DINA (15 nM)
TMZ + DINA
DAPI/CD44
DAPI/Ki67
DAPI/CC-3
B
Number of Nuclei
Control
TMZ
DINA
TMZ+DINA
C
Ki67
CD44
Cleaved Caspase-3
% Positive Cells
D
Heterogeneous GBM Population
Dinaciclib
CD44+
qRT-PCR
E
SPDYA
MAP2
Log10 RQ
Control
TMZ
DINA
TMZ + DINA

Figure 5: Dinaciclib decreases cell numbers and induces apoptosis in combination with TMZ.

(A) Representative images from immunocytochemistry of U251 cells stained with DAPI and antibodies for CD44, Ki67, and CC-3. Cells were treated with either 50 µM of DMSO as vehicle control (CONTROL), 50 µM of TMZ, 15 nM of dinaciclib (DINA) or a combination of both (50 µM TMZ + 15 nM DINA). Images were taken at 100x oil and scale bars represent 40 µm. (B) Total number of nuclei from each group was quantified using images taken at 20x and ImageJ. Error bars represent standard error of the mean from 5 different images taken. ***$p<0.001$. Statistical significance calculated using a one-way ANOVA. (C) Percentage of cells positively stained for each antibody of Ki67, CD44, and CC-3. Total number of cells were counted using the same method as (B) and cells stained for each antibody was counted in the same method under Texas red filter image. Error bars represent standard error from 5 collected data points from 5 separate images. *$p<0.05$, **$p<0.005$, ***$p<0.001$. Statistical significance was calculated using a one-way ANOVA. (D) Schematic of $CD44^+$ cells being isolated from dinaciclib treatment and mRNA levels tested with qRT-PCR. Image created with biorender.com. (E) Log_{10} Relative Quantity (RQ) of *SPDYA* and *MAP2* mRNA levels in U251 cells.

3. Total Foci are Reduced *in vivo* with Dinaciclib Treatment

A schematic of the workflow for zebrafish injections is presented in Figure 6. Drugs tested in zebrafish embryos are shown in Table 1, and dinaciclib demonstrated the lowest amount of lethality and was therefore selected to be used. U87 cells were fluorescently labelled and injected into anesthetized embryos. Successfully injected embryos were treated with a high and a low concentration of dinaciclib, 75 nM and 7.5 nM, respectively. Images were taken daily of all embryos up until 7dpi (Figure 7A). Total foci area was measured using the raw integrated intensity from ImageJ analysis. Each group was then normalized to itself starting at 3dpi, the time when drug treatment ended. At 4dpi there was a significant decrease of the foci area when the high concentration of dinaciclib was used, compared to the low concentration, but the decrease was not significant when compared to the DMSO treated control fish. However, at 7dpi, there was a significant decrease in foci area in the high concentration of dinaciclib compared to both the control and the low concentration of dinaciclib (Figure 7B). In summary, it was found that dinaciclib was less toxic to embryos and caused a decrease in total foci *in vivo* compared to the vehicle control.

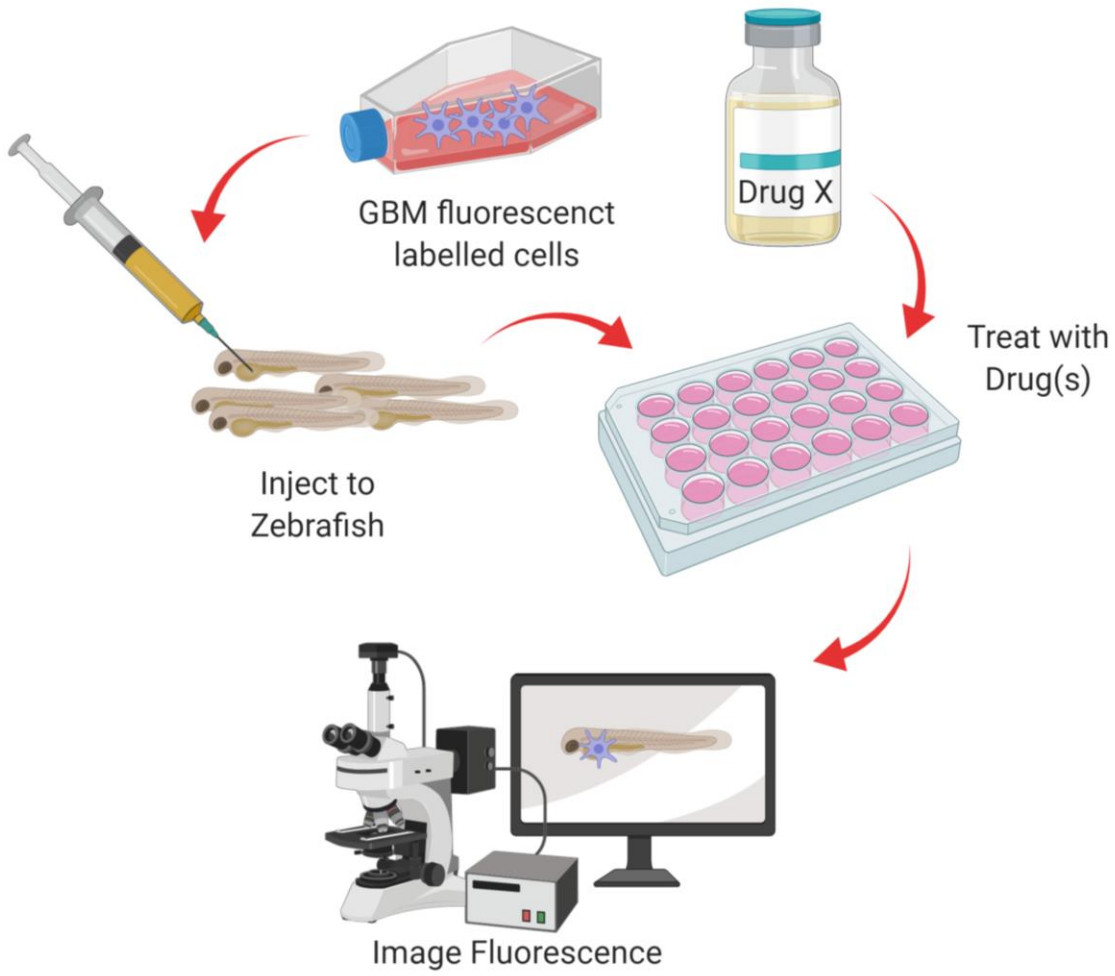

Figure 6: Schematic of zebrafish injections.

(A) GBM cells were labelled with fluorescent dye and injected into anesthetized zebrafish embryos 2 days old. (B) Fish were placed in a 12-well plate at 8 fish per well. Fish were imaged and screened 24 hours after injection to select successfully injected fish to be subsequently moved to a new plate. (C) Drug treatments and vehicle control were added 24 hours after injection. (D) Images were taken using an inverted microscope (Leica) every day before each treatment. Image created with biorender.com

Table 1: Drug viability in zebrafish embryos

Treatment	Concentration		
dinaciclib[§]	25 nM	250 nM	1000 nM
Total Embryos	50	50	50
Embryos Alive	50	49	50
% Death	0	2	0
DMSO Vehicle Control	*	*	*
Total Embryos	50	50	50
Embryos Alive	49	49	48
% Death	2	2	4
————————————————————————————			
NU2058[§]	25 µM	50 µM	100 µM
Total Embryos	55	54	56
Embryos Alive	35	33	2
% Death	36.36	38.89	92.86
DMSO Vehicle Control	*	*	*
Total Embryos	54	55	55
Embryos Alive	51	54	53
% Death	5.55	1.82	3.63
————————————————————————————			
TMZ[†]	40 µM	125 µM	250 µM
Total Embryos	30	30	30
Embryos Alive	30	29	30
% Death	0	3.33	0
DMSO Vehicle Control	*	*	*
Total Embryos	N/A	N/A	30
Embryos Alive	N/A	N/A	27
% Death	N/A	N/A	10

* DMSO vehicle control was matched in dilution to media to corresponding drug treatment

§ Result of 2 separate experiments

† Only one replicate completed, vehicle control only done at one concentration

A

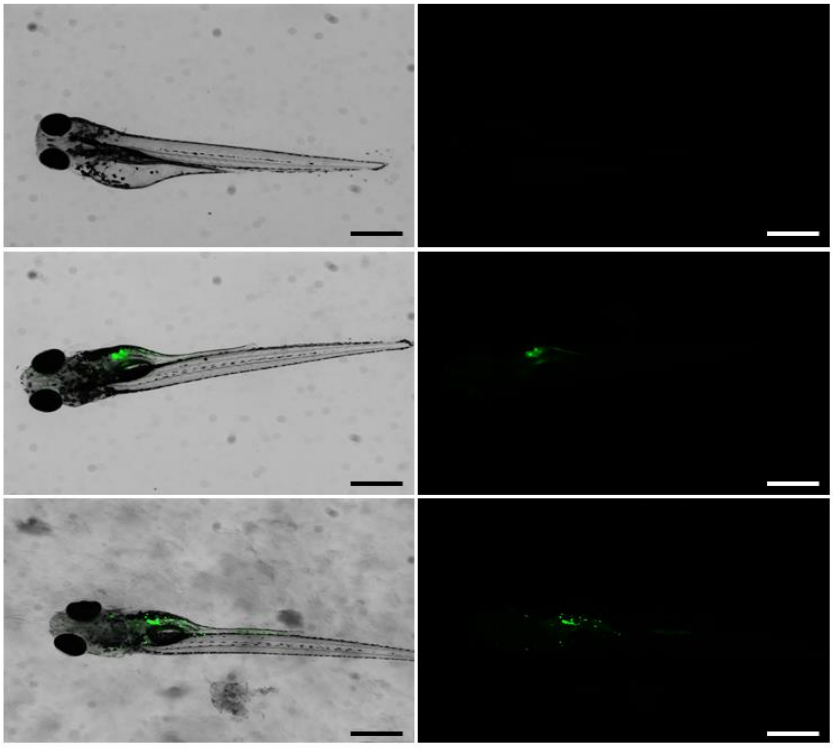
Day 1
Day 3
Day 7

B

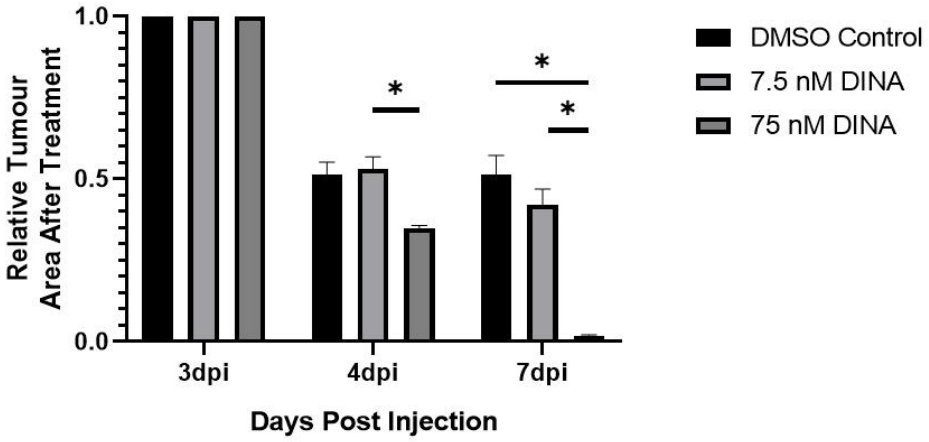
Relative Tumour Area After Treatment
1.0
0.5
0.0
3dpi
4dpi
7dpi
Days Post Injection
*
*
*
DMSO Control
7.5 nM DINA
75 nM DINA

Figure 7: Dinaciclib reduces relative tumour area.

(A) Representative fluorescent and overlay images of zebrafish used for analysis. Embryos were anesthetized with Tricaine and injected with U87 cells. Scale bars equal 500 µm. Top image represents a sham injected embryo. (B) Tumour area was measured at 3, 4, and 7dpi. Tumour area was normalized to 3dpi, the day treatments ended. Intensity of foci was measured using ImageJ. Error bars represent the standard error from 2 groups, each group representing at least 6 fish. *$p<0.05$. Statistical significance was calculated using multiple Student's t-tests.

4. Dinaciclib Reduces Metastases Proximal to the Brain

Images taken at 7dpi were also analyzed for metastases proximal to the brain. Fish that had foci past the swim bladder, towards the eyes and away from the point of injection (yolk sac/intestines) and appeared to be near the brain (see Figure 1A) were quantified as fish with metastases proximal to brain. Figure 8A shows representative images from the DMSO vehicle control group with foci of U87 cells which were declared as fish with metastases proximal to the brain (red arrows). Each treatment group was measured this way and then total fish with metastases proximal to the brain were put into a percentage of the total amount of fish in that treatment group. Although there was no significance between groups, there is a trend of decreased metastasis towards the brain as dinaciclib concentration increases (Figure 8B). Images from the DMSO control group and no treatment (NT) group were then analyzed for total brain metastases and total tail metastases and then compared to untreated 3dpi embryos injected with breast cancer cells (MDA-MB-231). Tail metastases were measured by foci detected past the swim bladder (see Figure 1A). There were significantly more metastases proximal to the brain in fish injected with the U87 cell line, and a significant increase in tail metastases in fish injected with the MDA-MB-231 cell line (Figure 8C). Representative fluorescent and overlay image of a fish injected with U87 cells with tail metastases can be seen in Figure 8D. Although more work is needed as validation, it would appear the U87 cell line preferentially migrates towards the brain, and dinaciclib reduces this metastasis *in vivo*.

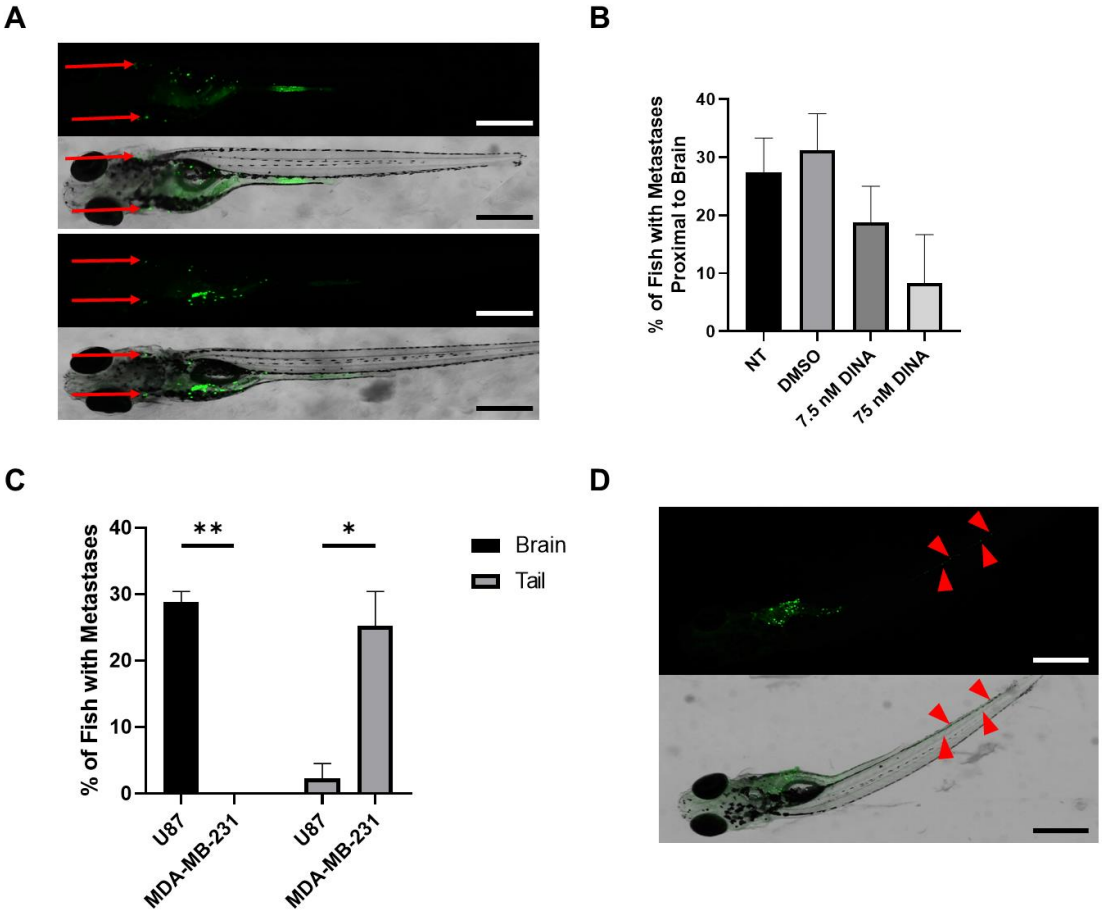
A
B
% of Fish with Metastases Proximal to Brain
40
30
20
10
0
NT
DMSO
7.5 nM DINA
75 nM DINA
C
% of Fish with Metastases
**
*
Brain
Tail
U87
MDA-MB-231
U87
MDA-MB-231
D

Figure 8: Dinaciclib reduces metastasis towards the brain.

(A) Representative fluorescent and overlay images of 7dpi zebrafish. U87 foci (red arrows) show metastasis in the vicinity of the midbrain and hindbrain. Both images are from the DMSO vehicle control group. Scale bars equals 500 μm. (B) Images were analyzed and put into categories of no metastases proximal to brain and metastases proximal to brain. There was no significance between groups according to a one-way ANOVA. NT = no treatment, DMSO = vehicle control, DINA = dinaciclib. Error bars represent the standard error from 2 groups, each group representing at least 6 fish. (C) All 7dpi fish from NT and DMSO groups were analyzed for brain and tail metastases, and additional images of the breast cancer cell line MDA-MB-231 cells injected into the yolk sac were obtained from Janice Tubman and analyzed for brain and tail metastases. Images analyzed from Janice Tubman were taken at 3dpi. Error bars represent the standard of error from 2 groups, each group containing at least 16 fish. *$p<0.05$, **$p<0.005$. Statistical significance was calculated using a 2-way ANOVA. (D) Representative fluorescent and overlay images of 7dpi zebrafish injected with U87 cells. U87 foci (red arrowheads) show metastasis down the tail. Both images are from the DMSO vehicle control group. Scale bars equals 500 μm.

DISCUSSION

Since the introduction of TMZ over a decade ago, the standard of care for patients with GBM has not been challenged to advance the clinical outcomes leaving patient survival rates in the same dismal position (Cantrell et al., 2019). It is therefore important to continue to explore new treatment and therapy options, including novel drugs and drug combinations, to improve survival rates and quality of life for patients with GBM.

This study aimed to validate different combinations of CKIs and chemotherapy in the treatment of GBM *in vitro*. We found that all combinations of a CKI and chemotherapy tested caused high antagonism between the two drugs at most of the concentrations used in U251 cell line (Figure 4). The U87 cell line showed similar results, and although the combination of TMZ and NU2058 showed an overall additive effect, only 2 of the 9 matrix plots were tested significant, compared to 5 to 7 of 9 significant matrix plots of all other matrix plots for U87 cell line (Figure 3). Additionally, there were two EC_{50} values (TMZ and etoposide) that were determined through interpolation in the U87 cell line. We recognize that these drugs barely cause 50% inhibition in the U87 cell line, and this demonstrates the high chemoresistance of GBM. This emphasizes the need for synergistic drug interactions in GBM treatment, especially because these interpolated results come from the currently used chemotherapies and not from the experimental CKIs. The observed antagonistic relationship could potentially result from the counteractive mechanisms of action of the drugs tested. The CKIs work by inhibiting CDKs and subsequently the cell cycle, stopping cells from dividing and growing (Hardcastle et al., 2004; Parry et al., 2010; Sedlacek, 2001). However, typical chemotherapy agents work by targeting actively dividing cells, causing DNA damage

either directly or indirectly, leading to apoptosis (Chen, Chan, & Hsieh, 2013; Wilstermann et al., 2007; Wu et al., 2011; Zhang, Stevens, & Bradshaw, 2012). The timing of drug administration could be a major factor for the antagonism between a CKI and chemotherapy agent and should be further investigated. Recent work including bevacizumab, an angiogenesis inhibitor, addresses the issue of treatment timing in GBM patients in the clinic. Pasqualetti et al. showed that the timing of bevacizumab administration affected the median time of disease recurrence from the initial GBM diagnosis, from 9.9 months for early bevacizumab administration (after first line chemotherapy) to 13.1 months for delayed bevacizumab administration (after second- or third-line chemotherapy) (Pasqualetti et al., 2018). Although the overall survival rates were unchanged, this study shows that timing of bevacizumab administration may at least play a role in improving the quality of life for GBM patients.

In terms of CKI and chemotherapy treatment, the timing could be critical depending on the specific characteristics of the combined drugs. For example, if a chemotherapy agent causes DNA damage at the end of G_1 checkpoint or at mid S phase checkpoint, and a CKI causes a cell cycle stop at the G_2/M checkpoint, it may be more beneficial to treat with the chemotherapy agent first. This would allow for DNA damage to accumulate, for the subsequently applied CKI, to stop the cell cycle at the end of DNA accumulation, allowing for more time to detect DNA damage and for activation of appropriate molecular signals toward apoptosis. Alternatively, if the chemotherapy agent causes DNA damage late in the cell cycle, it may be more beneficial to first treat with a CKI, which stops the cell cycle early, allowing the cells to synchronize, followed by treating with the chemotherapy after the CKI has been metabolized. This approach may

result in optimizing the number of cells affected by the chemotherapy, increasing the cytotoxic effects and reducing chemoresistance.

Jane et al. showed that dinaciclib, in combination with Bcl-2/Bcl-xL inhibitors, significantly reduced GBM cell proliferation rates independent of p53 status, and there was little to no effect on cell population or apoptosis in the GBM cell line T98G when dinaciclib was combined with other chemotherapeutics, including TMZ and etoposide. However, a very high concentration of dinaciclib was used, at 1 µM, which is as much as 1000 times higher than the calculated IC_{50} values for the inhibition of CDK2 and CDK5 (1 nM). In addition, cells were only treated for 24 hours, limiting the time for cells to accumulate DNA damage and signal for apoptosis (Jane et al., 2016). These high concentrations of dinaciclib could be a factor in the results seen in combination treatments with other chemotherapeutics. It has been demonstrated recently that dinaciclib in low concentrations (5 nM), in combination with doxorubicin, enhanced senescence in the multiple myeloma cell line RPMI-8226 (Tang, Xu, Liang, & Gao, 2018). The data presented by Jane et al. is consistent with this work; dinaciclib alone causes growth inhibition, but not cell death, in GBM cells. Our data show that cultures treated with dinaciclib alone and in combination with TMZ significantly reduced the total number of cells (Figure 5B). Furthermore, our study is the first to characterize the post-dinaciclib treatment cell populations. The remaining cells demonstrate more stem-like and aggressive character with elevated protein expression of stem-cell marker CD44 and proliferation marker Ki67, as well as increased transcript levels of BTIC expansion marker *SPDYA* and decreased transcript levels of the differentiation marker *MAP2*. These results suggest that dinaciclib selects for and leaves behind aggressive and drug resistant

cell populations. This particular outcome of dinaciclib treatment could potentially serve as an important strategy for combination therapy as it selects BTIC population to be specifically targeted by another agent, limiting the expansion of the cells at the same time. Further work is needed, however, to determine the role of administration timing as well as potential agents to cooperate with the BTIC selective nature of dinaciclib. In summary, our and published data show that other parameters such as timing and mechanism of action along with drug concentration, play a pivotal role in the anticancer action of combined agents and should be carefully investigated while designing treatment regimens.

To address the effects of combination therapy *in vivo*, we utilized zebrafish xenograft and drug testing model. Despite several advantages of utilizing zebrafish there are many controversies about the model for cancer research. One large disadvantage in tumour transplantation using zebrafish is the temperature difference. Zebrafish embryos are maintained at 28°C, a large gap from the human body at 37°C. Most researchers compromise proper development of the embryo and optimal growth temperatures of the tumour cells, by exposing both embryos and xenografted cells to an "in-between" temperature, ranging from 32.5-35°C (Barriuso, Nagaraju, & Hurlstone, 2015; Cabezas-Sainz et al., 2018; Kirchberger, Sturtzel, Pascoal, & Distel, 2017). A recent study by Cabezas-Sainz et al. suggests that injection and maintenance at 36°C optimizes cell growth and has no significant effect on the development of the embryo when compared to 34°C (Cabezas-Sainz et al., 2018). Yan et al. also showed a transgenic zebrafish model that could maintain normal function at 37°C and could be xenografted with a large number of different human cancers (Yan et al., 2019). In this study, embryos were kept at

28°C upon collection for 1 day, where they were subsequently moved to 33°C for the remainder of the experiments.

Additionally, zebrafish are not an ideal model for human diseases that take place in specific organs of the human body that zebrafish do not have, including prostate, breast, and lungs (Kirchberger, Sturtzel, Pascoal, & Distel, 2017). Despite those limitations, zebrafish offers cancer studies in a high-throughput manner, where human cells can be readily xenografted at certain immunocompromised stages of zebrafish development into an *in vivo* microenvironment (Greaves & Maley, 2012; Wertman, Veinotte, Dellaire, & Berman, 2016). Standard drug treatment of zebrafish embryos involves adding the drug to the water the embryos are in, which results in drugs taken up passively through the skin of the embryos (Kari, Rodeck, & Dicker, 2007). It is possible to measure the amount of drug absorbed by the zebrafish embryos using liquid chromatography-tandem mass spectrometry (Chen et al., 2017; Zhang, Qin, Zhang, & Hu, 2015). However, there is currently no way to measure the exact amount of drug being metabolized by zebrafish embryos.

Figure 6 is a graphical abstract of the method used in this thesis to inject and collect data from the zebrafish embryos. This method involved using groups of embryos in a larger well and analyzing the averages of the groups. It is not uncommon that other researchers look at each fish individually, and each method has its own advantages and disadvantages. When looking at each fish individually, each fish is placed in a single well of a 96-well plate creating a high-throughput study platform (Basnet, Zizioli, Taweedet, Finazzi, & Memo, 2019; Ferraiuolo, Tubman, Sinha, Hamm, & Porter, 2017; Lambert et al., 2018). Although technically advantageous, this adds multiple layers of stress on the

embryo, which includes the small size of the well and feeding the fish in small confined space causing increased ammonia levels and an increased pH. In a smaller space these toxicities would theoretically accumulate faster due to the smaller volume of water. A major concern at this point is supplying the nutrition to the embryo but keeping them under consistent and not compromised environment during drug treatment. It is well established that the yolk is fully diminished by ~7dpf, and it is essential that the embryos are fed from this point on, but ideally 1-2 days before (Mathias, Saxena, & Mumm, 2012). The time required for establishing tumour foci and tumour mass significantly exceeds that range of time, making it essential to keep the embryos fed. Using a 96-well plate to study zebrafish embryos individually is much more beneficial when comparing each fish individually over time during toxicity screens and for live imaging at the single cell level (White et al., 2008). When using zebrafish embryos for drug screening one can make the case for a larger well and pooling groups of embryos and averaging the results. By using a less stressful environment the embryos are healthier and subjected to more consistent environment with less possibility for an error.

The potential toxic effects of two CKIs, dinaciclib and NU2058, were tested on zebrafish embryos. Dinaciclib was non-toxic in the embryos at concentrations as high as 89-fold higher than the calculated EC_{50} values in the GBM cell lines used. Comparatively, NU2058 was extremely toxic to the embryos at concentrations close to the EC_{50} values, making it a poor drug to move forward with drug screening using zebrafish embryos (Table 1). NU2058 is an experimental drug not seen in recent literature, suggesting that the toxicity of this drug to animal models quickly eliminated it from use in research. On the other hand, dinaciclib is still being used today in clinical

trials. When zebrafish embryos were injected with U87 cells and subsequently treated with dinaciclib, there was a significant decrease in foci area in high concentration (75 nM) compared to vehicle control (DMSO) or low concentration (7.5 nM) after 4 days from the last treatment (Figure 7B). This would suggest that dinaciclib had successfully caused growth inhibition of injected U87 cells in the embryos, which is consistent with what is seen *in vitro*. The same embryo images were used in analysis of metastases of U87 cells (Figure 8). Although there were no significant differences seen (Figure 8B), there is a trend demonstrating that dinaciclib is reducing the total number of metastases towards the head. The limitations of this data are due to low replicate numbers (n=2), and future work would include the addition of more replicates as well as the addition of more GBM cell lines as well as patient-derived cell lines. Of the fish injected with U87 cells, the DMSO vehicle control and no treatment groups had a high percentage of fish with metastases proximal to the brain, but when analyzed for tail metastases, there were very few. Images of 3dpi embryos, injected with MDA-MB-231 cells (a breast cancer cell line), were obtained from Janice Tubman and analyzed the same way as the U87 cell injected embryos for brain and tail metastases. Interestingly there were no metastases proximal to the brain, but many down the tail (Figure 8C). This data would suggest that the human GBM cells are preferentially migrating towards the brain, confirming the validity of zebrafish as an animal model. The human MDA-MB-231 cells are a known invasive cell line, and there is evidence of those cells metastasizing throughout the zebrafish embryo once injected, including to the brain, eye, and tail, but no data on the amount of fish with specific metastases (Tulotta et al., 2016). There is also evidence of those cells metastasizing to the bone in zebrafish embryos (Mercatali et al., 2016). As

high as 70% of breast and prostate cancer patients with relapse develop bone metastases (Ibrahim, Mercatali, & Amadori, 2013; Mercatali et al., 2016; Roodman, 2004), and, as mentioned above, zebrafish lack specific organs that humans have, such as prostate, breast, and lungs (Kirchberger, Sturtzel, Pascoal, & Distel, 2017). The fact that the breast cancer cell line MDA-MB-231 tends to metastasize down the tail is interesting, and the lack of breasts within the zebrafish is of further interest. Future work would be needed to test this, for example, injecting zebrafish embryos with different types of human cancers, some with common organs (brain and liver), and some without (breast and prostate), and quantifying the amount of metastasis and localization of that metastasis. This experiment could solidify the use of zebrafish as an animal model for cancer, and potentially put some controversies to rest. This experiment would require sectioning and staining of zebrafish in order to confirm the localization of the transplanted cells. This highlights more future work required for this thesis, sectioning and staining injected zebrafish embryos to determine if the U87 cell line had in fact metastasized to the nervous tissue.

In conclusion, this thesis has demonstrated that dinaciclib, in concurrent combination with a chemotherapy, is antagonistic in the GBM cell lines U87 and U251, and dinaciclib inhibits GBM cell growth and selects for the BTIC population *in vitro*. This advocates the potential use of dinaciclib in treatment of GBM, in combination with a treatment targeting the $CD44^+$ BTIC population, and also addresses the question of the timing of drug treatments in the clinic, especially in clinical trials involving CKIs.

REFERENCES/BIBLIOGRAPHY

Agarwala, S. S., & Kirkwood, J. M. (2000). Temozolomide, a novel alkylating agent with activity in the central nervous system, may improve the treatment of advanced metastatic melanoma. *The Oncologist*, *5*(2), 144–151. https://doi.org/10.1634/theoncologist.5-2-144

Al-Hajj, M., Wicha, M. S., Benito-Hernandez, A., Morrison, S. J., & Clarke, M. F. (2003). Prospective identification of tumorigenic breast cancer cells. *Proceedings of the National Academy of Sciences of the United States of America*, *100*(7), 3983–3988. https://doi.org/10.1073/pnas.0530291100

Arellano, M., & Moreno, S. (1997). Regulation of CDK/cyclin complexes during the cell cycle. *The International Journal of Biochemistry & Cell Biology*, *29*(4), 559–573.

Arris, C. E., Boyle, F. T., Calvert, A. H., Curtin, N. J., Endicott, J. A., Garman, E. F., … Yu, W. (2000). Identification of novel purine and pyrimidine cyclin-dependent kinase inhibitors with distinct molecular interactions and tumor cell growth inhibition profiles. *Journal of Medicinal Chemistry*, *43*(15), 2797–2804. https://doi.org/10.1021/jm990628o

Asnani, A., & Peterson, R. T. (2014). The zebrafish as a tool to identify novel therapies for human cardiovascular disease. *Disease Models & Mechanisms*, *7*(7), 763–767. https://doi.org/10.1242/dmm.016170

Bailon-Moscoso, N., Cevallos-Solorzano, G., Romero-Benavides, J. C., & Orellana, M. I. R. (2017). Natural Compounds as Modulators of Cell Cycle Arrest: Application for Anticancer Chemotherapies. *Current Genomics*, *18*(2), 106–131. https://doi.org/10.2174/1389202917666160808125645

Barnes, E. A., Porter, L. A., Lenormand, J.-L., Dellinger, R. W., & Donoghue, D. J. (2003). Human Spy1 promotes survival of mammalian cells following DNA damage. *Cancer Research*, *63*(13), 3701–3707.

Barriuso, J., Nagaraju, R., & Hurlstone, A. (2015). Zebrafish: A new companion for translational research in oncology. *Clinical Cancer Research : An Official Journal of the American Association for Cancer Research*, *21*(5), 969–975. https://doi.org/10.1158/1078-0432.CCR-14-2921

Basnet, R. M., Zizioli, D., Taweedet, S., Finazzi, D., & Memo, M. (2019). Zebrafish Larvae as a Behavioral Model in Neuropharmacology. *Biomedicines*, *7*(1). https://doi.org/10.3390/biomedicines7010023

Baumann, M., Krause, M., & Hill, R. (2008). Exploring the role of cancer stem cells in radioresistance. *Nature Reviews. Cancer*, *8*(7), 545–554. https://doi.org/10.1038/nrc2419

Begicevic, R.-R., & Falasca, M. (2017). ABC Transporters in Cancer Stem Cells: Beyond Chemoresistance. *International Journal of Molecular Sciences*, *18*(11). https://doi.org/10.3390/ijms18112362

Besson, A., Gurian-West, M., Schmidt, A., Hall, A., & Roberts, J. M. (2004). P27Kip1 modulates cell migration through the regulation of RhoA activation. *Genes & Development*, *18*(8), 862–876. https://doi.org/10.1101/gad.1185504

Bliss, C. I. (1939). The Toxicity of Poisons Applied Jointly. *Annals of Applied Biology*, *26*(3), 585–615. https://doi.org/10.1111/j.1744-7348.1939.tb06990.x

Bradshaw, A., Wickremesekera, A., Brasch, H. D., Chibnall, A. M., Davis, P. F., Tan, S. T., & Itinteang, T. (2016). Cancer Stem Cells in Glioblastoma Multiforme. *Frontiers in Surgery*, *3*, 48. https://doi.org/10.3389/fsurg.2016.00048

Bronner, S. M., Merrick, K. A., Murray, J., Salphati, L., Moffat, J. G., Pang, J., … Heffron, T. P. (2019). Design of a brain-penetrant CDK4/6 inhibitor for glioblastoma. *Bioorganic & Medicinal Chemistry Letters*, *29*(16), 2294–2301. https://doi.org/10.1016/j.bmcl.2019.06.021

Brown, D. V., Filiz, G., Daniel, P. M., Hollande, F., Dworkin, S., Amiridis, S., … Mantamadiotis, T. (2017). Expression of CD133 and CD44 in glioblastoma stem cells correlates with cell proliferation, phenotype stability and intra-tumor heterogeneity. *PloS One*, *12*(2), e0172791. https://doi.org/10.1371/journal.pone.0172791

Bundgaard, M., & Abbott, N. J. (2008). All vertebrates started out with a glial blood-brain barrier 4-500 million years ago. *Glia*, *56*(7), 699–708. https://doi.org/10.1002/glia.20642

Cabezas-Sainz, P., Guerra-Varela, J., Carreira, M. J., Mariscal, J., Roel, M., Rubiolo, J. A., … Sanchez, L. (2018). Improving zebrafish embryo xenotransplantation conditions by increasing incubation temperature and establishing a proliferation index with ZFtool. *BMC Cancer*, *18*(1), 3. https://doi.org/10.1186/s12885-017-3919-8

Canepa, E. T., Scassa, M. E., Ceruti, J. M., Marazita, M. C., Carcagno, A. L., Sirkin, P. F., & Ogara, M. F. (2007). INK4 proteins, a family of mammalian CDK inhibitors with novel biological functions. *IUBMB Life*, *59*(7), 419–426. https://doi.org/10.1080/15216540701488358

Cantrell, J. N., Waddle, M. R., Rotman, M., Peterson, J. L., Ruiz-Garcia, H., Heckman, M. G., … Trifiletti, D. M. (2019). Progress Toward Long-Term Survivors of Glioblastoma. *Mayo Clinic Proceedings*, *94*(7), 1278–1286. https://doi.org/10.1016/j.mayocp.2018.11.031

Cardoso, F. L., Brites, D., & Brito, M. A. (2010). Looking at the blood-brain barrier: Molecular anatomy and possible investigation approaches. *Brain Research Reviews, 64*(2), 328–363. https://doi.org/10.1016/j.brainresrev.2010.05.003

Carnero, A., & Hannon, G. J. (1998). The INK4 family of CDK inhibitors. *Current Topics in Microbiology and Immunology*, *227*, 43–55.

Carpentier, A., Canney, M., Vignot, A., Reina, V., Beccaria, K., Horodyckid, C., … Idbaih, A. (2016). Clinical trial of blood-brain barrier disruption by pulsed ultrasound. *Science Translational Medicine*, *8*(343), 343re2. https://doi.org/10.1126/scitranslmed.aaf6086

Chen, B., Gao, Z.-Q., Liu, Y., Zheng, Y.-M., Han, Y., Zhang, J.-P., & Hu, C.-Q. (2017). Embryo and Developmental Toxicity of Cefazolin Sodium Impurities in Zebrafish. *Frontiers in Pharmacology*, *8*, 403. https://doi.org/10.3389/fphar.2017.00403

Chen, S. H., Chan, N.-L., & Hsieh, T. (2013). New mechanistic and functional insights into DNA topoisomerases. *Annual Review of Biochemistry*, *82*, 139–170. https://doi.org/10.1146/annurev-biochem-061809-100002

Cheng, C. K., Gustafson, W. C., Charron, E., Houseman, B. T., Zunder, E., Goga, A., … Fan, Q.-W. (2012). Dual blockade of lipid and cyclin-dependent kinases induces synthetic lethality in malignant glioma. *Proceedings of the National Academy of Sciences of the United States of America*, *109*(31), 12722–12727. https://doi.org/10.1073/pnas.1202492109

Cheung, Z. H., & Ip, N. Y. (2012). Cdk5: A multifaceted kinase in neurodegenerative diseases. *Trends in Cell Biology*, *22*(3), 169–175. https://doi.org/10.1016/j.tcb.2011.11.003

Chi, N. C., Shaw, R. M., Jungblut, B., Huisken, J., Ferrer, T., Arnaout, R., … Stainier, D. Y. R. (2008). Genetic and physiologic dissection of the vertebrate cardiac conduction system. *PLoS Biology*, *6*(5), e109. https://doi.org/10.1371/journal.pbio.0060109

Chou, T. C., & Talalay, P. (1977). A simple generalized equation for the analysis of multiple inhibitions of Michaelis-Menten kinetic systems. *The Journal of Biological Chemistry*, *252*(18), 6438–6442.

Comprehensive genomic characterization defines human glioblastoma genes and core pathways. (2008). *Nature*, *455*(7216), 1061–1068. https://doi.org/10.1038/nature07385

Coqueret, O. (2003). New roles for p21 and p27 cell-cycle inhibitors: A function for each cell compartment? *Trends in Cell Biology*, *13*(2), 65–70.

Di Veroli, G. Y., Fornari, C., Wang, D., Mollard, S., Bramhall, J. L., Richards, F. M., & Jodrell, D. I. (2016). Combenefit: An interactive platform for the analysis and visualization of drug combinations. *Bioinformatics (Oxford, England)*, *32*(18), 2866–2868. https://doi.org/10.1093/bioinformatics/btw230

Domb, A. J., Rock, M., Perkin, C., Yipchuck, G., Broxup, B., & Villemure, J. G. (1995). Excretion of a radiolabelled anticancer biodegradable polymeric implant from the rabbit brain. *Biomaterials*, *16*(14), 1069–1072. https://doi.org/10.1016/0142-9612(95)98902-q

Eagan, R. T., Carr, D. T., Frytak, S., Rubin, J., & Lee, R. E. (1976). VP-16-213 versus polychemotherapy in patients with advanced small cell lung cancer. *Cancer Treatment Reports*, *60*(7), 949–951.

Einhorn, L. H. (1990). Treatment of testicular cancer: A new and improved model. *Journal of Clinical Oncology : Official Journal of the American Society of Clinical Oncology*, *8*(11), 1777–1781. https://doi.org/10.1200/JCO.1990.8.11.1777

Evans, A., Scher, C., & D'Angio, G. (1992). Treatment of advanced neuroblastoma. *European Journal of Cancer (Oxford, England : 1990)*, *28A*(8–9), 1301–1302. https://doi.org/10.1016/0959-8049(92)90502-s

Eyler, C. E., & Rich, J. N. (2008). Survival of the fittest: Cancer stem cells in therapeutic resistance and angiogenesis. *Journal of Clinical Oncology : Official Journal of the American Society of Clinical Oncology*, *26*(17), 2839–2845. https://doi.org/10.1200/JCO.2007.15.1829

Ferby, I., Blazquez, M., Palmer, A., Eritja, R., & Nebreda, A. R. (1999). A novel p34(cdc2)-binding and activating protein that is necessary and sufficient to trigger G(2)/M progression in Xenopus oocytes. *Genes & Development*, *13*(16), 2177–2189. https://doi.org/10.1101/gad.13.16.2177

Ferraiuolo, R.-M., Tubman, J., Sinha, I., Hamm, C., & Porter, L. A. (2017). The cyclin-like protein, SPY1, regulates the ERalpha and ERK1/2 pathways promoting tamoxifen resistance. *Oncotarget*, *8*(14), 23337–23352. https://doi.org/10.18632/oncotarget.15578

Firestein, R., Bass, A. J., Kim, S. Y., Dunn, I. F., Silver, S. J., Guney, I., … Hahn, W. C. (2008). CDK8 is a colorectal cancer oncogene that regulates beta-catenin activity. *Nature*, *455*(7212), 547–551. https://doi.org/10.1038/nature07179

Fleming, A., Diekmann, H., & Goldsmith, P. (2013). Functional characterisation of the maturation of the blood-brain barrier in larval zebrafish. *PloS One*, *8*(10), e77548. https://doi.org/10.1371/journal.pone.0077548

Foucquier, J., & Guedj, M. (2015). Analysis of drug combinations: Current methodological landscape. *Pharmacology Research & Perspectives*, *3*(3), e00149. https://doi.org/10.1002/prp2.149

Ghotra, V. P. S., He, S., de Bont, H., van der Ent, W., Spaink, H. P., van de Water, B., … Danen, E. H. J. (2012). Automated whole animal bio-imaging assay for human cancer dissemination. *PloS One*, *7*(2), e31281. https://doi.org/10.1371/journal.pone.0031281

Gibert, Y., Trengove, M. C., & Ward, A. C. (2013). Zebrafish as a genetic model in pre-clinical drug testing and screening. *Current Medicinal Chemistry*, *20*(19), 2458–2466. https://doi.org/10.2174/0929867311320190005

Gilbert, M. R., Friedman, H. S., Kuttesch, J. F., Prados, M. D., Olson, J. J., Reaman, G. H., & Zaknoen, S. L. (2002). A phase II study of temozolomide in patients with newly diagnosed supratentorial malignant glioma before radiation therapy. *Neuro-Oncology*, *4*(4), 261–267. https://doi.org/10.1093/neuonc/4.4.261

Gilbert, M. R., Wang, M., Aldape, K. D., Stupp, R., Hegi, M. E., Jaeckle, K. A., … Mehta, M. P. (2013). Dose-dense temozolomide for newly diagnosed glioblastoma: A randomized phase III clinical trial. *Journal of Clinical Oncology : Official Journal of the American Society of Clinical Oncology*, *31*(32), 4085–4091. https://doi.org/10.1200/JCO.2013.49.6968

Girard, F., Strausfeld, U., Fernandez, A., & Lamb, N. J. (1991). Cyclin A is required for the onset of DNA replication in mammalian fibroblasts. *Cell*, *67*(6), 1169–1179. https://doi.org/10.1016/0092-8674(91)90293-8

Goldstone, J. V., McArthur, A. G., Kubota, A., Zanette, J., Parente, T., Jonsson, M. E., … Stegeman, J. J. (2010). Identification and developmental expression of the full

complement of Cytochrome P450 genes in Zebrafish. *BMC Genomics*, *11*, 643. https://doi.org/10.1186/1471-2164-11-643

Greaves, M., & Maley, C. C. (2012). Clonal evolution in cancer. *Nature*, *481*(7381), 306–313. https://doi.org/10.1038/nature10762

Greco, W. R., Bravo, G., & Parsons, J. C. (1995). The search for synergy: A critical review from a response surface perspective. *Pharmacological Reviews*, *47*(2), 331–385.

Groothuis, D. R. (2000). The blood-brain and blood-tumor barriers: A review of strategies for increasing drug delivery. *Neuro-Oncology*, *2*(1), 45–59. https://doi.org/10.1093/neuonc/2.1.45

Haldi, M., Ton, C., Seng, W. L., & McGrath, P. (2006). Human melanoma cells transplanted into zebrafish proliferate, migrate, produce melanin, form masses and stimulate angiogenesis in zebrafish. *Angiogenesis*, *9*(3), 139–151. https://doi.org/10.1007/s10456-006-9040-2

Hanahan, D., & Weinberg, R. A. (2011). Hallmarks of cancer: The next generation. *Cell*, *144*(5), 646–674. https://doi.org/10.1016/j.cell.2011.02.013

Hardcastle, I. R., Arris, C. E., Bentley, J., Boyle, F. T., Chen, Y., Curtin, N. J., … Whitfield, H. J. (2004). N2-substituted O6-cyclohexylmethylguanine derivatives: Potent inhibitors of cyclin-dependent kinases 1 and 2. *Journal of Medicinal Chemistry*, *47*(15), 3710–3722. https://doi.org/10.1021/jm0311442

Harper, J. W., Elledge, S. J., Keyomarsi, K., Dynlacht, B., Tsai, L. H., Zhang, P., … Swindell, E. (1995). Inhibition of cyclin-dependent kinases by p21. *Molecular Biology of the Cell*, *6*(4), 387–400. https://doi.org/10.1091/mbc.6.4.387

Hegi, M. E., Diserens, A.-C., Gorlia, T., Hamou, M.-F., de Tribolet, N., Weller, M., … Stupp, R. (2005). MGMT gene silencing and benefit from temozolomide in glioblastoma. *The New England Journal of Medicine*, *352*(10), 997–1003. https://doi.org/10.1056/NEJMoa043331

Hemmati, H. D., Nakano, I., Lazareff, J. A., Masterman-Smith, M., Geschwind, D. H., Bronner-Fraser, M., & Kornblum, H. I. (2003). Cancerous stem cells can arise from pediatric brain tumors. *Proceedings of the National Academy of Sciences of the United States of America*, *100*(25), 15178–15183. https://doi.org/10.1073/pnas.2036535100

Hengst, L., & Reed, S. I. (1998). Inhibitors of the Cip/Kip family. *Current Topics in Microbiology and Immunology*, *227*, 25–41.

Higginbottom, K., Cummings, M., Newland, A. C., & Allen, P. D. (2002). Etoposide-mediated deregulation of the G2M checkpoint in myeloid leukaemic cell lines results in loss of cell survival. *British Journal of Haematology*, *119*(4), 956–964. https://doi.org/10.1046/j.1365-2141.2002.03977.x

Howe, K., Clark, M. D., Torroja, C. F., Torrance, J., Berthelot, C., Muffato, M., … Stemple, D. L. (2013). The zebrafish reference genome sequence and its relationship to the human genome. *Nature*, *496*(7446), 498–503. https://doi.org/10.1038/nature12111

Ibrahim, T., Mercatali, L., & Amadori, D. (2013). A new emergency in oncology: Bone metastases in breast cancer patients (Review). *Oncology Letters*, *6*(2), 306–310. https://doi.org/10.3892/ol.2013.1372

Iorns, E., Turner, N. C., Elliott, R., Syed, N., Garrone, O., Gasco, M., … Ashworth, A. (2008). Identification of CDK10 as an important determinant of resistance to endocrine therapy for breast cancer. *Cancer Cell*, *13*(2), 91–104. https://doi.org/10.1016/j.ccr.2008.01.001

Jane, E. P., Premkumar, D. R., Cavaleri, J. M., Sutera, P. A., Rajasekar, T., & Pollack, I. F. (2016). Dinaciclib, a Cyclin-Dependent Kinase Inhibitor Promotes Proteasomal Degradation of Mcl-1 and Enhances ABT-737-Mediated Cell Death in Malignant Human Glioma Cell Lines. *The Journal of Pharmacology and Experimental Therapeutics*, *356*(2), 354–365. https://doi.org/10.1124/jpet.115.230052

Jia, Jia, Zhu, F., Ma, X., Cao, Z., Cao, Z. W., Li, Y., … Chen, Y. Z. (2009). Mechanisms of drug combinations: Interaction and network perspectives. *Nature Reviews. Drug Discovery*, *8*(2), 111–128. https://doi.org/10.1038/nrd2683

Jia, Jianwu, Wang, J., Yin, M., & Liu, Y. (2019). MicroRNA-605 directly targets SOX9 to alleviate the aggressive phenotypes of glioblastoma multiforme cell lines by deactivating the PI3K/Akt pathway. *OncoTargets and Therapy*, *12*, 5437–5448. https://doi.org/10.2147/OTT.S213026

Johansen, A., Hansen, H. D., Svarer, C., Lehel, S., Leth-Petersen, S., Kristensen, J. L., … Knudsen, G. M. (2018). The importance of small polar radiometabolites in molecular neuroimaging: A PET study with [(11)C]Cimbi-36 labeled in two positions. *Journal of Cerebral Blood Flow and Metabolism : Official Journal of the International Society of Cerebral Blood Flow and Metabolism*, *38*(4), 659–668. https://doi.org/10.1177/0271678X17746179

Johansson, M., & Persson, J. L. (2008). Cancer therapy: Targeting cell cycle regulators. *Anti-Cancer Agents in Medicinal Chemistry*, *8*(7), 723–731.

Kari, G., Rodeck, U., & Dicker, A. P. (2007). Zebrafish: An emerging model system for human disease and drug discovery. *Clinical Pharmacology and Therapeutics*, *82*(1), 70–80. https://doi.org/10.1038/sj.clpt.6100223

Kastan, M. B., & Bartek, J. (2004). Cell-cycle checkpoints and cancer. *Nature*, *432*(7015), 316–323. https://doi.org/10.1038/nature03097

Kaur, G., Stetler-Stevenson, M., Sebers, S., Worland, P., Sedlacek, H., Myers, C., … Sausville, E. (1992). Growth inhibition with reversible cell cycle arrest of carcinoma cells by flavone. *Journal of the National Cancer Institute*, *84*(22), 1736–1740. https://doi.org/10.1093/jnci/84.22.1736

Kim, E. S. (2017). Abemaciclib: First Global Approval. *Drugs*, *77*(18), 2063–2070. https://doi.org/10.1007/s40265-017-0840-z

Kim, W. Y., & Sharpless, N. E. (2006). The regulation of INK4/ARF in cancer and aging. *Cell*, *127*(2), 265–275. https://doi.org/10.1016/j.cell.2006.10.003

Kirchberger, S., Sturtzel, C., Pascoal, S., & Distel, M. (2017). Quo natas, Danio?-Recent Progress in Modeling Cancer in Zebrafish. *Frontiers in Oncology*, *7*, 186. https://doi.org/10.3389/fonc.2017.00186

Kolenda, J., Jensen, S. S., Aaberg-Jessen, C., Christensen, K., Andersen, C., Brunner, N., & Kristensen, B. W. (2011). Effects of hypoxia on expression of a panel of stem cell and chemoresistance markers in glioblastoma-derived spheroids. *Journal of Neuro-Oncology*, *103*(1), 43–58. https://doi.org/10.1007/s11060-010-0357-8

Konantz, M., Balci, T. B., Hartwig, U. F., Dellaire, G., Andre, M. C., Berman, J. N., & Lengerke, C. (2012). Zebrafish xenografts as a tool for in vivo studies on human cancer. *Annals of the New York Academy of Sciences*, *1266*, 124–137. https://doi.org/10.1111/j.1749-6632.2012.06575.x

Kreso, A., & Dick, J. E. (2014). Evolution of the cancer stem cell model. *Cell Stem Cell*, *14*(3), 275–291. https://doi.org/10.1016/j.stem.2014.02.006

Lam, S. H., Chua, H. L., Gong, Z., Lam, T. J., & Sin, Y. M. (2004). Development and maturation of the immune system in zebrafish, Danio rerio: A gene expression profiling, in situ hybridization and immunological study. *Developmental and Comparative Immunology*, *28*(1), 9–28.

Lambert, C. J., Freshner, B. C., Chung, A., Stevenson, T. J., Bowles, D. M., Samuel, R., … Bonkowsky, J. L. (2018). An automated system for rapid cellular extraction from live zebrafish embryos and larvae: Development and application to genotyping. *PloS One*, *13*(3), e0193180. https://doi.org/10.1371/journal.pone.0193180

Lampreht Tratar, U., Horvat, S., & Cemazar, M. (2018). Transgenic Mouse Models in Cancer Research. *Frontiers in Oncology*, *8*, 268. https://doi.org/10.3389/fonc.2018.00268

Lee, L. M. J., Seftor, E. A., Bonde, G., Cornell, R. A., & Hendrix, M. J. C. (2005). The fate of human malignant melanoma cells transplanted into zebrafish embryos: Assessment of migration and cell division in the absence of tumor formation. *Developmental Dynamics : An Official Publication of the American Association of Anatomists*, *233*(4), 1560–1570. https://doi.org/10.1002/dvdy.20471

Lee, M. H., Reynisdottir, I., & Massague, J. (1995). Cloning of p57KIP2, a cyclin-dependent kinase inhibitor with unique domain structure and tissue distribution. *Genes & Development*, *9*(6), 639–649. https://doi.org/10.1101/gad.9.6.639

Lenormand, J. L., Dellinger, R. W., Knudsen, K. E., Subramani, S., & Donoghue, D. J. (1999). Speedy: A novel cell cycle regulator of the G2/M transition. *The EMBO Journal*, *18*(7), 1869–1877. https://doi.org/10.1093/emboj/18.7.1869

Li, C., Heidt, D. G., Dalerba, P., Burant, C. F., Zhang, L., Adsay, V., … Simeone, D. M. (2007). Identification of pancreatic cancer stem cells. *Cancer Research*, *67*(3), 1030–1037. https://doi.org/10.1158/0008-5472.CAN-06-2030

Li, J., Qian, W.-P., & Sun, Q.-Y. (2019). Cyclins regulating oocyte meiotic cell cycle progression. *Biology of Reproduction*. https://doi.org/10.1093/biolre/ioz143

Liebner, S., Czupalla, C. J., & Wolburg, H. (2011). Current concepts of blood-brain barrier development. *The International Journal of Developmental Biology*, *55*(4–5), 467–476. https://doi.org/10.1387/ijdb.103224sl

Lieschke, G. J., & Trede, N. S. (2009). Fish immunology. *Current Biology : CB*, *19*(16), R678-682. https://doi.org/10.1016/j.cub.2009.06.068

Lim, S., & Kaldis, P. (2013). Cdks, cyclins and CKIs: Roles beyond cell cycle regulation. *Development (Cambridge, England)*, *140*(15), 3079–3093. https://doi.org/10.1242/dev.091744

Liu, L., Michowski, W., Inuzuka, H., Shimizu, K., Nihira, N. T., Chick, J. M., … Sicinski, P. (2017). G1 cyclins link proliferation, pluripotency and differentiation of embryonic stem cells. *Nature Cell Biology*, *19*(3), 177–188. https://doi.org/10.1038/ncb3474

Loewe, S. (1928). Die quantitativen Probleme der Pharmakologie. *Ergebnisse Der Physiologie*, *27*(1), 47–187. https://doi.org/10.1007/BF02322290

Lotsch, J., & Geisslinger, G. (2011). Low-dose drug combinations along molecular pathways could maximize therapeutic effectiveness while minimizing collateral adverse effects. *Drug Discovery Today*, *16*(23–24), 1001–1006. https://doi.org/10.1016/j.drudis.2011.10.003

Louis, D. N., Perry, A., Reifenberger, G., von Deimling, A., Figarella-Branger, D., Cavenee, W. K., … Ellison, D. W. (2016). The 2016 World Health Organization Classification of Tumors of the Central Nervous System: A summary. *Acta Neuropathologica*, *131*(6), 803–820. https://doi.org/10.1007/s00401-016-1545-1

Lubanska, D., Market-Velker, B. A., deCarvalho, A. C., Mikkelsen, T., Fidalgo da Silva, E., & Porter, L. A. (2014). The cyclin-like protein Spy1 regulates growth and division characteristics of the CD133+ population in human glioma. *Cancer Cell*, *25*(1), 64–76. https://doi.org/10.1016/j.ccr.2013.12.006

Lubanska, D., & Porter, L. (2017). Revisiting CDK Inhibitors for Treatment of Glioblastoma Multiforme. *Drugs in R&D*, *17*(2), 255–263. https://doi.org/10.1007/s40268-017-0180-1

MacRae, C. A., & Peterson, R. T. (2015). Zebrafish as tools for drug discovery. *Nature Reviews. Drug Discovery*, *14*(10), 721–731. https://doi.org/10.1038/nrd4627

Martin, M. P., Olesen, S. H., Georg, G. I., & Schonbrunn, E. (2013). Cyclin-dependent kinase inhibitor dinaciclib interacts with the acetyl-lysine recognition site of bromodomains. *ACS Chemical Biology*, *8*(11), 2360–2365. https://doi.org/10.1021/cb4003283

Mathias, J. R., Saxena, M. T., & Mumm, J. S. (2012). Advances in zebrafish chemical screening technologies. *Future Medicinal Chemistry*, *4*(14), 1811–1822. https://doi.org/10.4155/fmc.12.115

Meijer, A. H., & Spaink, H. P. (2011). Host-pathogen interactions made transparent with the zebrafish model. *Current Drug Targets*, *12*(7), 1000–1017. https://doi.org/10.2174/138945011795677809

Mercatali, L., La Manna, F., Groenewoud, A., Casadei, R., Recine, F., Miserocchi, G., … Snaar-Jagalska, E. (2016). Development of a Patient-Derived Xenograft (PDX) of Breast

Cancer Bone Metastasis in a Zebrafish Model. *International Journal of Molecular Sciences*, *17*(8). https://doi.org/10.3390/ijms17081375

Minniti, G., Muni, R., Lanzetta, G., Marchetti, P., & Enrici, R. M. (2009). Chemotherapy for glioblastoma: Current treatment and future perspectives for cytotoxic and targeted agents. *Anticancer Research*, *29*(12), 5171–5184.

Molenaar, J. J., Ebus, M. E., Geerts, D., Koster, J., Lamers, F., Valentijn, L. J., … Caron, H. N. (2009). Inactivation of CDK2 is synthetically lethal to MYCN over-expressing cancer cells. *Proceedings of the National Academy of Sciences of the United States of America*, *106*(31), 12968–12973. https://doi.org/10.1073/pnas.0901418106

Morikawa, A., & Henry, N. L. (2015). Palbociclib for the Treatment of Estrogen Receptor-Positive, HER2-Negative Metastatic Breast Cancer. *Clinical Cancer Research : An Official Journal of the American Association for Cancer Research*, *21*(16), 3591–3596. https://doi.org/10.1158/1078-0432.CCR-15-0390

Mullard, A. (2017). FDA approves Novartis's CDK4/6 inhibitor. *Nature Reviews. Drug Discovery*, *16*(4), 229. https://doi.org/10.1038/nrd.2017.62

Mullins, M. C., Hammerschmidt, M., Haffter, P., & Nusslein-Volhard, C. (1994). Large-scale mutagenesis in the zebrafish: In search of genes controlling development in a vertebrate. *Current Biology : CB*, *4*(3), 189–202. https://doi.org/10.1016/s0960-9822(00)00048-8

Nam, C., Doi, K., & Nakayama, H. (2010). Etoposide induces G2/M arrest and apoptosis in neural progenitor cells via DNA damage and an ATM/p53-related pathway. *Histology and Histopathology*, *25*(4), 485–493. https://doi.org/10.14670/HH-25.485

Nemunaitis, J. J., Small, K. A., Kirschmeier, P., Zhang, D., Zhu, Y., Jou, Y.-M., … Bannerji, R. (2013). A first-in-human, phase 1, dose-escalation study of dinaciclib, a novel cyclin-

dependent kinase inhibitor, administered weekly in subjects with advanced malignancies. *Journal of Translational Medicine*, *11*, 259. https://doi.org/10.1186/1479-5876-11-259

Norbury, C., & Nurse, P. (1992). Animal cell cycles and their control. *Annual Review of Biochemistry*, *61*, 441–470. https://doi.org/10.1146/annurev.bi.61.070192.002301

O'Brown, N. M., Pfau, S. J., & Gu, C. (2018). Bridging barriers: A comparative look at the blood-brain barrier across organisms. *Genes & Development*, *32*(7–8), 466–478. https://doi.org/10.1101/gad.309823.117

Ohtsubo, M., Theodoras, A. M., Schumacher, J., Roberts, J. M., & Pagano, M. (1995). Human cyclin E, a nuclear protein essential for the G1-to-S phase transition. *Molecular and Cellular Biology*, *15*(5), 2612–2624. https://doi.org/10.1128/mcb.15.5.2612

Ortega, S., Malumbres, M., & Barbacid, M. (2002). Cyclin D-dependent kinases, INK4 inhibitors and cancer. *Biochimica et Biophysica Acta*, *1602*(1), 73–87. https://doi.org/10.1016/s0304-419x(02)00037-9

Otto, T., & Sicinski, P. (2017). Cell cycle proteins as promising targets in cancer therapy. *Nature Reviews. Cancer*, *17*(2), 93–115. https://doi.org/10.1038/nrc.2016.138

Pardridge, W. M. (2005). The blood-brain barrier: Bottleneck in brain drug development. *NeuroRx : The Journal of the American Society for Experimental NeuroTherapeutics*, *2*(1), 3–14. https://doi.org/10.1602/neurorx.2.1.3

Pardridge, W. M. (2009). Alzheimer's disease drug development and the problem of the blood-brain barrier. *Alzheimer's & Dementia : The Journal of the Alzheimer's Association*, *5*(5), 427–432. https://doi.org/10.1016/j.jalz.2009.06.003

Parry, D., Guzi, T., Shanahan, F., Davis, N., Prabhavalkar, D., Wiswell, D., … Lees, E. M. (2010). Dinaciclib (SCH 727965), a novel and potent cyclin-dependent kinase inhibitor.

Molecular Cancer Therapeutics, *9*(8), 2344–2353. https://doi.org/10.1158/1535-7163.MCT-10-0324

Pasqualetti, F., Gonnelli, A., Molinari, A., Cantarella, M., Montrone, S., Cristaudo, A., … Paiar, F. (2018). Different Timing to Use Bevacizumab in Patients with Recurrent Glioblastoma: Early Versus Delayed Administration. *Anticancer Research*, *38*(10), 5877–5881. https://doi.org/10.21873/anticanres.12930

Pemovska, T., Bigenzahn, J. W., & Superti-Furga, G. (2018). Recent advances in combinatorial drug screening and synergy scoring. *Current Opinion in Pharmacology*, *42*, 102–110. https://doi.org/10.1016/j.coph.2018.07.008

Polyak, K., Lee, M. H., Erdjument-Bromage, H., Koff, A., Roberts, J. M., Tempst, P., & Massague, J. (1994). Cloning of p27Kip1, a cyclin-dependent kinase inhibitor and a potential mediator of extracellular antimitogenic signals. *Cell*, *78*(1), 59–66. https://doi.org/10.1016/0092-8674(94)90572-x

Porter, L. A., Dellinger, R. W., Tynan, J. A., Barnes, E. A., Kong, M., Lenormand, J.-L., & Donoghue, D. J. (2002). Human Speedy: A novel cell cycle regulator that enhances proliferation through activation of Cdk2. *The Journal of Cell Biology*, *157*(3), 357–366. https://doi.org/10.1083/jcb.200109045

Quintavalle, M., Elia, L., Price, J. H., Heynen-Genel, S., & Courtneidge, S. A. (2011). A cell-based high-content screening assay reveals activators and inhibitors of cancer cell invasion. *Science Signaling*, *4*(183), ra49. https://doi.org/10.1126/scisignal.2002032

Rahman, R., Hempfling, K., Norden, A. D., Reardon, D. A., Nayak, L., Rinne, M. L., … Lee, E. Q. (2014). Retrospective study of carmustine or lomustine with bevacizumab in

recurrent glioblastoma patients who have failed prior bevacizumab. *Neuro-Oncology*, *16*(11), 1523–1529. https://doi.org/10.1093/neuonc/nou118

Rello-Varona, S., Fuentes-Guirado, M., Lopez-Alemany, R., Contreras-Perez, A., Mulet-Margalef, N., Garcia-Monclus, S., … Garcia Del Muro, X. (2019). Bcl-xL inhibition enhances Dinaciclib-induced cell death in soft-tissue sarcomas. *Scientific Reports*, *9*(1), 3816. https://doi.org/10.1038/s41598-019-40106-7

Rigas, A. C., Robson, C. N., & Curtin, N. J. (2007). Therapeutic potential of CDK inhibitor NU2058 in androgen-independent prostate cancer. *Oncogene*, *26*(55), 7611–7619. https://doi.org/10.1038/sj.onc.1210586

Roel, M., Rubiolo, J. A., Guerra-Varela, J., Silva, S. B. L., Thomas, O. P., Cabezas-Sainz, P., … Botana, L. M. (2016). Marine guanidine alkaloids crambescidins inhibit tumor growth and activate intrinsic apoptotic signaling inducing tumor regression in a colorectal carcinoma zebrafish xenograft model. *Oncotarget*, *7*(50), 83071–83087. https://doi.org/10.18632/oncotarget.13068

Roodman, G. D. (2004). Mechanisms of bone metastasis. *The New England Journal of Medicine*, *350*(16), 1655–1664. https://doi.org/10.1056/NEJMra030831

Roskoski, R. J. (2019). Cyclin-dependent protein serine/threonine kinase inhibitors as anticancer drugs. *Pharmacological Research*, *139*, 471–488. https://doi.org/10.1016/j.phrs.2018.11.035

Roussel, M. F. (1999). The INK4 family of cell cycle inhibitors in cancer. *Oncogene*, *18*(38), 5311–5317. https://doi.org/10.1038/sj.onc.1202998

Sedlacek, H. H. (2001). Mechanisms of action of flavopiridol. *Critical Reviews in Oncology/Hematology*, *38*(2), 139–170.

Seliger, C., & Hau, P. (2018). Drug Repurposing of Metabolic Agents in Malignant Glioma. *International Journal of Molecular Sciences*, *19*(9). https://doi.org/10.3390/ijms19092768

Senbanjo, L. T., & Chellaiah, M. A. (2017). CD44: A Multifunctional Cell Surface Adhesion Receptor Is a Regulator of Progression and Metastasis of Cancer Cells. *Frontiers in Cell and Developmental Biology*, *5*, 18. https://doi.org/10.3389/fcell.2017.00018

Shapira-Furman, T., Serra, R., Gorelick, N., Doglioli, M., Tagliaferri, V., Cecia, A., … Domb, A. J. (2019). Biodegradable wafers releasing Temozolomide and Carmustine for the treatment of brain cancer. *Journal of Controlled Release : Official Journal of the Controlled Release Society*, *295*, 93–101. https://doi.org/10.1016/j.jconrel.2018.12.048

Sharma, P. S., Sharma, R., & Tyagi, R. (2008). Inhibitors of cyclin dependent kinases: Useful targets for cancer treatment. *Current Cancer Drug Targets*, *8*(1), 53–75.

Shen, S., Dean, D. C., Yu, Z., & Duan, Z. (2019). Role of cyclin-dependent kinases (CDKs) in hepatocellular carcinoma: Therapeutic potential of targeting the CDK signaling pathway. *Hepatology Research : The Official Journal of the Japan Society of Hepatology*. https://doi.org/10.1111/hepr.13353

Sherr, C. J. (1994). G1 phase progression: Cycling on cue. *Cell*, *79*(4), 551–555. https://doi.org/10.1016/0092-8674(94)90540-1

Sherr, C. J., & Roberts, J. M. (1999). CDK inhibitors: Positive and negative regulators of G1-phase progression. *Genes & Development*, *13*(12), 1501–1512. https://doi.org/10.1101/gad.13.12.1501

Singh, S. K., Hawkins, C., Clarke, I. D., Squire, J. A., Bayani, J., Hide, T., … Dirks, P. B. (2004). Identification of human brain tumour initiating cells. *Nature*, *432*(7015), 396–401. https://doi.org/10.1038/nature03128

Spiro, Z., Kovacs, I. A., & Csermely, P. (2008). Drug-therapy networks and the prediction of novel drug targets. *Journal of Biology*, *7*(6), 20. https://doi.org/10.1186/jbiol81

Spitsbergen, J. (2007). Imaging neoplasia in zebrafish. *Nature Methods*, *4*(7), 548–549. https://doi.org/10.1038/nmeth0707-548

Stamatovic, S. M., Keep, R. F., & Andjelkovic, A. V. (2008). Brain endothelial cell-cell junctions: How to "open" the blood brain barrier. *Current Neuropharmacology*, *6*(3), 179–192. https://doi.org/10.2174/157015908785777210

Stoletov, K., Montel, V., Lester, R. D., Gonias, S. L., & Klemke, R. (2007). High-resolution imaging of the dynamic tumor cell vascular interface in transparent zebrafish. *Proceedings of the National Academy of Sciences of the United States of America*, *104*(44), 17406–17411. https://doi.org/10.1073/pnas.0703446104

Streisinger, G., Walker, C., Dower, N., Knauber, D., & Singer, F. (1981). Production of clones of homozygous diploid zebra fish (Brachydanio rerio). *Nature*, *291*(5813), 293–296. https://doi.org/10.1038/291293a0

Tang, H., Xu, L., Liang, X., & Gao, G. (2018). Low dose dinaciclib enhances doxorubicin-induced senescence in myeloma RPMI8226 cells by transformation of the p21 and p16 pathways. *Oncology Letters*, *16*(5), 6608–6614. https://doi.org/10.3892/ol.2018.9474

Tonder, M., Weller, M., Eisele, G., & Roth, P. (2014). Carboplatin and Etoposide in Heavily Pretreated Patients with Progressive High-Grade Glioma. *Chemotherapy*, *60*(5–6), 375–378. https://doi.org/10.1159/000440678

Traver, D., Herbomel, P., Patton, E. E., Murphey, R. D., Yoder, J. A., Litman, G. W., … Trede, N. S. (2003). The zebrafish as a model organism to study development of the immune system. *Advances in Immunology*, *81*, 253–330.

Tulotta, C., Stefanescu, C., Beletkaia, E., Bussmann, J., Tarbashevich, K., Schmidt, T., & Snaar-Jagalska, B. E. (2016). Inhibition of signaling between human CXCR4 and zebrafish ligands by the small molecule IT1t impairs the formation of triple-negative breast cancer early metastases in a zebrafish xenograft model. *Disease Models & Mechanisms*, *9*(2), 141–153. https://doi.org/10.1242/dmm.023275

Veinotte, C. J., Dellaire, G., & Berman, J. N. (2014). Hooking the big one: The potential of zebrafish xenotransplantation to reform cancer drug screening in the genomic era. *Disease Models & Mechanisms*, *7*(7), 745–754. https://doi.org/10.1242/dmm.015784

Vermeulen, K., Van Bockstaele, D. R., & Berneman, Z. N. (2003). The cell cycle: A review of regulation, deregulation and therapeutic targets in cancer. *Cell Proliferation*, *36*(3), 131–149. https://doi.org/10.1046/j.1365-2184.2003.00266.x

Walker, D. H., & Maller, J. L. (1991). Role for cyclin A in the dependence of mitosis on completion of DNA replication. *Nature*, *354*(6351), 314–317. https://doi.org/10.1038/354314a0

Wang, F., Cao, Y., Ma, L., Pei, H., Rausch, W. D., & Li, H. (2018). Dysfunction of Cerebrovascular Endothelial Cells: Prelude to Vascular Dementia. *Frontiers in Aging Neuroscience*, *10*, 376. https://doi.org/10.3389/fnagi.2018.00376

Wang, S., Yao, F., Lu, X., Li, Q., Su, Z., Lee, J.-H., … Du, L. (2019). Temozolomide promotes immune escape of GBM cells via upregulating PD-L1. *American Journal of Cancer Research*, *9*(6), 1161–1171.

Wang, Y. A., Elson, A., & Leder, P. (1997). Loss of p21 increases sensitivity to ionizing radiation and delays the onset of lymphoma in atm-deficient mice. *Proceedings of the National Academy of Sciences of the United States of America*, *94*(26), 14590–14595. https://doi.org/10.1073/pnas.94.26.14590

Weiss, R. B., & Issell, B. F. (1982). The nitrosoureas: Carmustine (BCNU) and lomustine (CCNU). *Cancer Treatment Reviews*, *9*(4), 313–330.

Wertman, J., Veinotte, C. J., Dellaire, G., & Berman, J. N. (2016). The Zebrafish Xenograft Platform: Evolution of a Novel Cancer Model and Preclinical Screening Tool. *Advances in Experimental Medicine and Biology*, *916*, 289–314. https://doi.org/10.1007/978-3-319-30654-4_13

Westerfield, M. (2000). *The zebrafish book. A guide for the laboratory use of zebrafish (Danio rerio).* (4th edition). Eugene, Oregon: Univ. of Oregon Press.

White, R. M., Sessa, A., Burke, C., Bowman, T., LeBlanc, J., Ceol, C., … Zon, L. I. (2008). Transparent adult zebrafish as a tool for in vivo transplantation analysis. *Cell Stem Cell*, *2*(2), 183–189. https://doi.org/10.1016/j.stem.2007.11.002

Williams, G. H., & Stoeber, K. (2012). The cell cycle and cancer. *The Journal of Pathology*, *226*(2), 352–364. https://doi.org/10.1002/path.3022

Wilstermann, A. M., Bender, R. P., Godfrey, M., Choi, S., Anklin, C., Berkowitz, D. B., … Graves, D. E. (2007). Topoisomerase II - drug interaction domains: Identification of substituents on etoposide that interact with the enzyme. *Biochemistry*, *46*(28), 8217–8225. https://doi.org/10.1021/bi700272u

Woolley, P. V., Dion, R. L., Kohn, K. W., & Bono, V. H. (1976). Binding of 1-(2-chloroethyl)-3-cyclohexyl-1-nitrosourea to L1210 cell nuclear proteins. *Cancer Research*, *36*(4), 1470–1474.

Wu, C.-C., Li, T.-K., Farh, L., Lin, L.-Y., Lin, T.-S., Yu, Y.-J., … Chan, N.-L. (2011). Structural basis of type II topoisomerase inhibition by the anticancer drug etoposide. *Science (New York, N.Y.)*, *333*(6041), 459–462. https://doi.org/10.1126/science.1204117

Xi, G., Hayes, E., Lewis, R., Ichi, S., Mania-Farnell, B., Shim, K., … Tomita, T. (2016). CD133 and DNA-PK regulate MDR1 via the PI3K- or Akt-NF-kappaB pathway in multidrug-resistant glioblastoma cells in vitro. *Oncogene*, *35*(42), 5576. https://doi.org/10.1038/onc.2016.64

Xing, W., Shao, C., Qi, Z., Yang, C., & Wang, Z. (2015). The role of Gliadel wafers in the treatment of newly diagnosed GBM: a meta-analysis. *Drug Design, Development and Therapy*, *9*, 3341–3348. https://doi.org/10.2147/DDDT.S85943

Zhang, F., Qin, W., Zhang, J.-P., & Hu, C.-Q. (2015). Antibiotic toxicity and absorption in zebrafish using liquid chromatography-tandem mass spectrometry. *PloS One*, *10*(5), e0124805. https://doi.org/10.1371/journal.pone.0124805

Zhang, J., Stevens, M. F. G., & Bradshaw, T. D. (2012). Temozolomide: Mechanisms of action, repair and resistance. *Current Molecular Pharmacology*, *5*(1), 102–114.

Zhao, H., Tang, C., Cui, K., Ang, B.-T., & Wong, S. T. C. (2009). A screening platform for glioma growth and invasion using bioluminescence imaging. Laboratory investigation. *Journal of Neurosurgery*, *111*(2), 238–246. https://doi.org/10.3171/2008.8.JNS08644

Zhao, W., Sachsenmeier, K., Zhang, L., Sult, E., Hollingsworth, R. E., & Yang, H. (2014). A New Bliss Independence Model to Analyze Drug Combination Data. *Journal of Biomolecular Screening*, *19*(5), 817–821. https://doi.org/10.1177/1087057114521867

Zhou, Y., Wu, S., Liang, C., Lin, Y., Zou, Y., Li, K., … Yan, G. (2015). Transcriptional upregulation of microtubule-associated protein 2 is involved in the protein kinase A-induced decrease in the invasiveness of glioma cells. *Neuro-Oncology*, *17*(12), 1578–1588. https://doi.org/10.1093/neuonc/nov060

Zimmer, N., Kim, E., Sprang, B., Leukel, P., Khafaji, F., Ringel, F., … Tuettenberg, A. (2019). GARP as an Immune Regulatory Molecule in the Tumor Microenvironment of Glioblastoma Multiforme. *International Journal of Molecular Sciences*, *20*(15). https://doi.org/10.3390/ijms20153676

VITA AUCTORIS

NAME:	Mathew Stover
PLACE OF BIRTH:	Chatham, ON
YEAR OF BIRTH:	1991
EDUCATION:	Tilbury District High School, Tilbury, ON, 2009
	The University of Western Ontario, B.M.Sc., London, ON, 2014